



ECG evaluation in early clinical trials

ECG evaluation as part of the clinical pharmacology
strategy in the development of new drugs

Darpo Borje, MD, PhD,
Borin, Marie, PhD,
Ferber Georg, PhD,
Galluppi, Gerald R, PhD,
Hopkins, Seth C, PhD,
Landry, Ishani, PhD,
Lo, Arthur, PhD,

Rege, Bhaskar, PhD,
Reyderman, Larisa, PhD,
Sun, Lei, PhD,
Watanabe, Takao, PhD,
Xue, Hongqi, PhD,
Yasuda, Sally, PhD

June 2022

ECG evaluation as part of the clinical pharmacology strategy in the development of new drugs

A review of current practices and opportunities based on 5 case studies

Darpo Borje, MD, PhD¹, Borin, Marie, PhD², Ferber Georg, PhD³, Galluppi, Gerald R, PhD⁴, Hopkins, Seth C, PhD⁴, Landry, Ishani, PhD⁵, Lo, Arthur, PhD², Rege, Bhaskar, PhD⁶, Reyderman, Larisa, PhD⁵, Sun, Lei, PhD⁶, Watanabe, Takao, PhD⁴, Xue, Hongqi, PhD¹, Yasuda, Sally, PhD⁵

1. Clario, Rochester, NY, USA
2. Clinical and Translational Pharmacology, Theravance Biopharma US, Inc., South San Francisco, CA, USA
3. Statistik Georg Ferber GmbH, Riehen, Switzerland
4. Sunovion Pharmaceuticals, Inc., USA
5. Clinical Pharmacology and Translational Medicine, Eisai, USA
6. Alkermes, Inc., Waltham, MA, USA

Corresponding author:

Borje Darpo, MD, PhD
Chief Scientific Officer Cardiac Safety,
Clario, 3750 Monroe Ave. Suite 600,
Pittsford, NY 14534, USA
Email: borje.darpo@telia.com
Telephone: +46 763 902 130

Short title: ECG evaluation in early clinical trials

Conflict of Interest: BD is Chief Scientific Officer of Clario and owns stock and is eligible for stock options in Clario. MB is a paid consultant for Theravance Biopharma.

Funding: There is no funding for this project.

Text: 7316 words; **Tables/Figures:** 1/11; **# references:** 31

This article has been accepted for publication and undergone full peer review but has not been through the copyediting, typesetting, pagination and proofreading process, which may lead to differences between this version and the [Version of Record](#). Please cite this article as [doi: 10.1111/jcph.2095](https://doi.org/10.1111/jcph.2095).

This article is protected by copyright. All rights reserved.

Abstract

The ICH E14 document was revised in 2015 to allow concentration-QTc (C-QTc) analysis to be applied to data from early clinical pharmacology studies to exclude a small drug-induced effect on the QTc interval. Provided sufficiently high concentrations of the drug are obtained in the First-in-Human (FIH) study, this approach can be used to obviate the need for a designated thorough QT (TQT) study. The E14 revision has resulted in a steady reduction in the number of TQT studies and increased use of FIH studies to evaluate ECG effects of drugs in development. In this publication, 5 examples from different sponsors are shared in which C-QTc analysis was performed on data from FIH studies. Case 1 illustrates a clearly negative C-QTc evaluation despite observations of QTc prolongation at high concentrations in non-clinical studies. In Case 2, C-QTc analysis of FIH data was performed prior to full pharmacokinetic characterization in patients and the role of non-clinical assays in an integrated risk assessment is discussed. Case 3 illustrates a positive clinical C-QTc relationship despite negative non-clinical assays. Case 4 shows a strategy for characterizing the C-QTc relationship for a non-racemic therapy and formulation optimization and Case 5 highlights an approach to perform a preliminary C-QTc analysis early in development and postpone the definitive analysis until proof-of-efficacy is demonstrated. The strategy of collecting and storing ECG data from FIH studies to enable an informed decision on whether and when to apply C-QTc analysis to obviate the need for a TQT study is described.

Max: 249 words (max 250)

Introduction

The 2015 revision of the ICH E14 Q&A document ^{1,2} was the result of an increasing confidence among regulators and sponsors in regard to using concentration-QTc (C-QTc) analysis to exclude small drug-induced effects on the QTc interval at the threshold of regulatory concern (10 msec) ^{3,4}. In addition, the IQ-CSRC study, conducted in collaboration between FDA, sponsors and the Cardiac Safety Research consortium (CSRC) and with full insight from other regulators, demonstrated that a study with only 9 subjects on active and 6 on placebo was able to detect and to exclude a QTc effect at this level, provided that sufficiently high doses of the drug were administered ⁵⁻⁷. Based on this, the revised Question 5.1 (Use of Concentration Response Modeling of QTc Data) in the E14 revision state that (extracted parts): *Concentration-response analysis, in which all available data across all doses are used to characterize the potential for a drug to influence QTc, can serve as an alternative to the by-time-point analysis or intersection-union test as the primary basis for decisions to classify the risk of a drug.* Under Important considerations: 2) *Efficient concentration-response analysis using data acquired in studies with other purposes requires as much quality control as is needed for a dedicated study. This includes robust, high-quality Electrocardiogram (ECG) recording and analysis sufficient to support a valid assay for ECG intervals (see E14 and Q&A #1); 4) If there are data characterizing the response at a sufficiently high multiple of the clinically relevant exposure (see E14 section 2.2.2), a separate positive control would not be necessary.* Finally, under Decision-making: *When using a concentration-response analysis as the primary basis for decisions to classify the risk of a drug, the upper bound of the two-sided 90% confidence interval for the QTc effect of a drug treatment as estimated by exposure-response analysis should be <10 ms at the highest clinically relevant exposure to conclude that an expanded ECG safety evaluation during later stages of drug development is not needed. (See E14, section 2.2.4 and Q&A #7).*

This revision opened a pathway for replacing the designated 'thorough QT (TQT) study' with evaluation of ECG data collected in clinical pharmacology studies, in which sufficiently high concentrations of the drug and its abundant metabolites were achieved. In most cases, this new emerging standard has been implemented in First-in-Human (FIH) studies, in which doses often are pushed to maximum tolerated doses (MTD). At the same time as the 2015 E14 revision was endorsed in all regions, studies were published that illustrated that C-QTc analysis applied to FIH trials could replace the regulatory need for a stand-alone TQT study ^{8,9}. As an example, lemborexant is indicated for treatment of insomnia and was approved by FDA in December 2019. In the development program, C-QTc analysis was implemented in 2 multiple-ascending-dose (MAD) studies; one conducted after completion of SAD and the second to bridge pharmacokinetics (PK) and safety into a Japanese population. Six dose groups with 8 healthy subjects in each (2 on placebo) with doses between 2.5 and 75 mg lemborexant were evaluated in the first MAD study. Three dose groups were evaluated in Japanese subjects and one in non-Japanese (at 10 mg) in the bridging study. Dosing was once daily in the evening 30 minutes before habitual bedtime for 14 days. Serial ECG monitoring paired with PK blood sampling was implemented in both studies. Replicate 12-lead ECGs were extracted from continuous ECG recordings (Holters) at time points at which subjects were supinely resting, as prespecified in the protocols. In **Figure 1**, the result from the C-QTc analysis performed on data pooled from these 2 studies is shown. The slope of the C-QTc relationship was very shallow and not statistically significant: -0.00002 msec per ng/mL (90% confidence interval (CI):

–0.0102 to 0.01014). As shown by the upper bound of the 90% CI, an effect on the QTc interval exceeding 10 msec could be excluded within the full plasma concentration range of lemborexant, i.e., up to more than 500 ng/mL. Importantly, therapeutic concentrations of this drug are around 40 to 60 ng/mL. When these data were shown to regulators in US and in Japan, the program was allowed to proceed into late-stage development without performing a TQT study and lemborexant was subsequently approved in these jurisdictions. The US label, therefore, states, under Cardiac Electrophysiology: *In a concentration-QTcF analysis using the data from two randomized, double-blind, placebo-controlled, multiple ascending dose studies in healthy subjects, lemborexant does not prolong the QTcF interval to any clinically relevant extent at a dose 5 times the maximum recommended dose.*

In this publication, we share 5 examples from different sponsors on how ECG evaluation can be implemented in FIH studies, with the objective to exclude clinically relevant effects on the QTc interval. To some extent, the examples represent different strategies for ECG evaluation in early clinical pharmacology studies, but all share the objective of potentially obviating the need for a designated, stand-alone TQT study.

- Case 1 illustrates a clear negative C-QTc relationship despite observations of QTc prolongation at high concentrations in non-clinical studies;
- Case 2 demonstrates the potential use of non-clinical studies to support a negative C-QTc relationship prior to the characterization of the high clinical exposure scenario;
- Case 3 illustrates a positive clinical C-QTc relationship despite negative non-clinical assays;
- Case 4 shows a strategy for characterizing the C-QTc relationship for a non-racemic therapy and formulation optimization, and
- Case 5 highlights a strategic methodology to plan and incorporate C-QTc analysis early in development.

Application of concentration-QTc (C-QTc) analysis

The relationship between plasma concentrations and Δ QTc is usually investigated using a linear mixed-effects modeling approach based on the model proposed by Garnett et al 2018¹⁰. This model has change-from-baseline QTc (Δ QTc) as the dependent variable, plasma concentrations as the explanatory variate (zero for placebo), centered baseline QTc (i.e., baseline QTc for individual subject minus the population mean baseline QTc for all subjects for parallel/single ascending dose (SAD)/MAD studies, and for all subjects within the same treatment period for crossover studies) as an additional covariate, study treatment (active = 1 or placebo = 0) and time (i.e., post-baseline time point) as fixed effects, and random effects on intercept and slope per subject. The relationship between plasma concentrations of major metabolites and Δ QTc is also investigated if metabolite concentration data are available. The full model with all of these analytes (parent drug and metabolites) and reduced models from possible first order combinations among these analytes may be explored and then a model selection procedure is usually undertaken, using the Akaike Information Criterion (AIC) to choose the primary model^{11,12}. In general, an unstructured covariance matrix is specified for the random effects. The degrees of freedom (*df*) estimates are determined by the Kenward-Roger method¹³. Several simplifications may be used if convergence of the full model cannot be achieved.

The key parameters to be estimated from such a model are the slope, i.e., the regression coefficient for concentration and the treatment specific intercept. In particular, the latter is also an important indicator for adequacy of the selected model, since an intercept that is significantly different from zero would imply a difference between a subject on placebo and one on active even for very low concentrations, a result that lacks biological plausibility. These two parameters (the slope and the intercept) are also the basis for the prediction of the effect of the drug on the QTc interval at concentrations of interest. Predictions are often made at the geometric mean (GM) maximum plasma concentration (C_{\max}) in each dose group, but more importantly, at clinically relevant concentrations, to the extent known. The model-predicted effect and its 2-sided 90% confidence interval (CI) for placebo-corrected ΔQTc ($\Delta\Delta\text{QTc} = \text{slope estimate} \times \text{concentration} + \text{treatment specific intercept}$) are presented. If the upper bound of the CI of this model-predicted QTc effect ($\Delta\Delta\text{QTc}$) is below 10 msec, the absence of an effect of regulatory concern at this concentration has been demonstrated.

Prior to fitting a model, it has to be ascertained that a proper correction method of the QT interval for heart rate was applied. This is particularly important if the drug also affects heart rate¹⁴. Following the guidance in the CSRC white paper on QT evaluation for drugs with a heart rate effect¹⁵, it is generally assumed that Fridericia's correction may be used if the drug does not affect heart rate by more than 10 bpm.

A second basic assumption of the type of models presented here is the absence of a delay between concentrations and the induced effect on the QTc interval. Such a delay will also be observed if the effect of the drug is caused by an active metabolite that appears later in plasma than the parent compound. In our case studies, hysteresis was assessed by graphical methods based on the least squares (LS) mean $\Delta\Delta\text{QTc}$ for each post-baseline time point in the by-time point analysis and mean concentrations at the same time points and by using so-called hysteresis loops¹⁰.

In regard to pooling data from more than one study, Garnett et al¹⁰ warn against pooling unless "control procedures (placebo, food)", ECG acquisition methods and the study population (comorbidities, concomitant medication) and, importantly, the conduct of studies are comparable. These conditions are best met if the studies to be pooled have been planned for this purpose upfront. When pooling, heterogeneity (unequal variance) should be assessed. For this purpose, plots of the standardized residuals versus fitted values of ΔQTcF and versus parts/studies based on the performance of the concentration-QTc models, and e.g., Levene's test for assessing the assumption of equal variances between the parts/studies can be used¹⁶.

Once a linear model has been fitted, the adequacy of model fit with respect to the assumption of linearity is investigated. For this, the use of quantile plots is recommended¹⁰: The observed ΔQTc values adjusted by population time effect estimated from the model (i.e., partial residuals) are used and a decile (10 equal sized bins) plot of observed drug concentrations and the mean $\Delta\Delta\text{QTc}$ and 90% CI within each decile is given. The regression line presenting the model-predicted $\Delta\Delta\text{QTc}$ (as described by Tornøe et al 2011¹⁷) is added to evaluate the fit of a linear model and visualize the concentration-response relationship. For pooled analyses the assumption of homogeneity (equal variances) is also assessed.

Case studies

[Table 1](#) summarizes key design features of included studies.

Case study 1 – Negative C-QTc evaluation that obviates the TQT study

E2027 is a novel, highly selective and potent inhibitor of phosphodiesterase-9 (PDE9) in development for dementia with Lewy bodies¹⁸.

E2027 inhibited human ether-à-go-go related gene (hERG) potassium currents concentration-dependently in hERG-transfected Chinese hamster ovary cells with an IC₅₀ value of 4.0 μM. In a conscious cynomolgus monkey cardiovascular (CV) study with oral administration of E2027 maleate, prolongation of corrected QT interval (QTc) and an increase in heart rate were observed at 300 and 1000 mg/kg. In a conscious monkey CV study with IV administration of E2027 (free base), increases in heart rate and maximum first derivative of left ventricular pressure (LVdP/dtmax) were observed at 10.8 and 24 mg/kg and a decrease in blood pressure was noted at 24 mg/kg. Decreases in body temperature, seen as indicating indicative of a central nervous system effect, were observed after 1000 mg/kg oral administration of E2027 maleate in rats, after 300 and 1000 mg/kg oral doses of E2027 maleate in monkeys and after a 24 mg/kg IV dose of E2027 (free base) in monkeys. The CV effects and hypothermia were observed at E2027 plasma concentrations of 5220 ng/mL and higher, which is ~6-fold higher than steady state C_{max} (C_{max_ss}) of the dose taken forward into phase 2 studies. Respiratory function was not affected at any dose in rats.

Concentration-QTc analysis was performed on data from two randomized, double-blind studies, each in healthy Japanese and non-Japanese subjects: a SAD study (NCT02415790) and a MAD study for 14 days (NCT02873156; **Table 1**). 12-lead ECGs were extracted in replicates from continuous Holter recordings prior to dosing and 0.5, 1, 2, 3, 4, 6, 8, 12 and 24 hours post-dose on Day 1 and at corresponding time points on Day -1 in both SAD and MAD and on Day 14 in MAD. In both studies, a time-matched baseline was used, i.e., values at corresponding time points on Day -1 served as baseline for post-dosing time points.

Profiles of change-from-baseline QTcF (ΔQTcF) and E2027 plasma concentration across dose groups and post-dosing time points are shown in **Figure 2, Panel A and B** (SAD) and **Panel C and D** (MAD). The pattern of mean ΔQTcF across active dose groups and placebo suggests that E2027 does not exert a meaningful effect on the QTc interval. Differences across post-dose time points between the time of C_{max} and the largest mean ΔΔQTcF were not consistent across dose groups with the highest concentrations and therefore did not suggest the presence of hysteresis. Substantial accumulation of E2027 plasma concentration was observed from Day 1 to Day 14, and the GM C_{max} level on Day 14 in the 400 mg daily dose group (2646 ng/mL) was therefore higher as compared to GM C_{max} in the 1200 mg single dose group (1736 ng/mL).

A scatter plot over pairs of observed E2027 plasma concentrations and ΔQTcF by race is shown in **Figure 3, panel A**. A linear mixed-effects model with a treatment specific intercept provided an acceptable fit to the observed data and was used to establish the relationship between plasma concentrations of E2027 and ΔQTcF (**Figure 3, Panel B**). A significant but shallow C-QTc relationship was observed with a slope of 0.002 msec per ng/mL (90% CI: 0.0007 to 0.0031) and a small, non-significant treatment specific intercept of -0.6 msec. An effect on the QTcF interval >10 msec could

be excluded up to E2027 plasma concentrations of ~3579 ng/mL, corresponding to a dose at least 4-fold larger than the 50 mg phase 2 dose. The goodness-of-fit plot suggests that the model provides an acceptable fit to the observed data. The highest concentrations of E2027 will be seen in patients who are taking the drug with food and have reduced clearance due to hepatic impairment or are also on concomitant medication with a potent 3A4 inhibitor (the *High Clinical Exposure* scenario). Mean C_{max_ss} in these patient groups can be estimated to be ~1300 ng/mL, which is almost 3-fold below concentration levels at which a QTc effect > 10 msec can be excluded using the C-QTc analysis from the SAD and MAD studies.

Case study 2 - Negative C-QTc evaluation prior to characterization of *High Clinical Exposure Scenario*

Compound 2 is a small molecule compound, which is in development for the treatment of central nervous system disorders.

Compound 2 was evaluated in human embryonic kidney cells stably expressing the hERG channel by a whole cell patch-clamp system. Compound 2 at concentrations of 30, 100, and 300 μ M inhibited hERG current in a concentration dependent manner, ranging from approximately 9% to 54% inhibition. IC₅₀ was calculated to 260.64 μ M. Prolongation of the QTc interval was observed in telemeterized dog and monkey CV studies at doses \geq 10 mg/kg. At this dose, a decrease in body temperature was also seen, an effect that has been reported to produce an increase in QTc¹⁹. In general, the QTc effects corresponded to the decrease in body temperature observed following Compound 2 administration and were considered secondary to this effect; however, at the highest dose levels (\geq 30 mg/kg), slightly larger effects on the QTc interval were seen, which could not be completely attributed to the decrease in body temperature. An increase in blood pressure and heart rate was also observed in rats, dogs, and monkeys at high doses, more pronounced in dogs than in monkeys.

Concentration-QTc analysis was applied to data from a double blind, placebo-controlled FIH SAD study in healthy adult subjects (**Table 1**). Twelve-lead ECGs were extracted from continuous recordings at -2 hours, -60, -45, and -15 minutes prior to dosing and 0.5, 1, 1.5, 2, 3, 4, 6, 8, 12, and 24 hours post-dose.

Compound 2 at the studied doses did not have a clinically relevant effect on heart rate or on cardiac conduction, i.e., the PR and QRS intervals. Profiles of Δ QTcF and Compound 2 plasma concentration across dose groups and post-dosing time points are shown in **Figure 4, panel A and B**. In the highest dose group (200 mg), there seemed to be a small effect, which did not correlate with plasma concentrations, with the largest mean Δ QTcF of 8.8 msec at 6 hours post-dose. The largest mean Δ QTcF between 1 and 4 hours post-dose in this dose group was 4.7 msec (at 3 hours), whereas mean values in all lower dose groups were \leq 0.6 msec. This pattern of mean Δ QTcF across doses and post-dose time points does not suggest a dose- or concentration-dependent effect. Geometric mean C_{max} levels in the 150 mg and 200 mg dose groups reached 389 and 466 ng/mL, respectively, with the highest values observed at 1.5 hours post-dose.

A scatter plot of observed Compound 2 plasma concentrations and Δ QTcF with linear and local regression (LOESS)²⁰ is shown in **Figure 5, Panel A**. There is little divergence between a simple linear

regression and the LOESS regression, which indicates that application of a linear C-QTc model is appropriate.

A linear mixed-effects model with a treatment specific intercept provided an acceptable fit to the observed QTcF data and was used to establish the relationship between plasma concentrations of Compound 2 and Δ QTcF (**Figure 5, Panel B**). A significant, but very shallow C-QTc relationship was observed with a slope of 0.0064 msec per ng/mL (90% CI: 0.00166 to 0.01110) and a small, non-significant treatment specific intercept of -0.9 msec. Using this C-QTc analysis, an effect on Δ QTcF exceeding 10 msec can be excluded within the full observed range of plasma concentrations of Compound 2 up to ~591 ng/mL. The PK profile of this drug is still being characterized in the targeted patient population, i.e., the *High Clinical Exposure scenario* is not yet defined. Studies are underway to determine the likelihood and extent of variability in drug exposure due to drug-drug interactions or in special populations.

Case study 3 - Clinical QTc Prolongation signal despite clean non-clinical assays

Case 3 is an example in which the sponsor made the decision to implement procedures for intense ECG evaluation in the FIH study and to analyze the data early in the development process, even though there was no expectation of ECG effects at predicted therapeutic exposure or at the exposures anticipated with the highest dose in SAD or MAD.

Cardiovascular evaluations following single dose administrations of Compound 3 in cynomolgus monkeys identified hemodynamic effects (decreased heart rate and increased blood pressure parameters) and ECG-related changes (increased interval durations and changes in waveform morphology). Decreases in heart rates were observed at doses ≥ 30 mg/kg, with changes at ≥ 60 mg/kg considered drug-related due to the magnitude of effect. Compensatory increases in ECG interval durations (PR, QRS, RR, and QT) were associated with decreases in heart rate and at doses up to 30 mg/kg, the magnitude of these changes was considered to be an expected physiological response. At doses above 60 mg/kg, prolongation of the QT interval corrected with the Bazett formula (QTcB), was seen. Since QTcB is known to underestimate the QTc effect when a drug reduces the heart rate, this can be seen as a conservative evaluation and with correction methods that better correct for underlying heart rate changes (e.g., QTcF and van de Waters), the effect would have been larger². At 300 mg/kg, increases in PR and QRS interval duration exceeded the expected physiological response to decreased heart rate, and mean QTcB was increased approximately 60 msec relative to control. The exposure at which adverse CV findings were observed in monkeys were ≥ 39 -fold and ≥ 19 -fold above C_{max} and AUC, respectively, of the projected efficacious human exposure. These effects could not be readily explained by effects of either Compound 3 or its primary metabolite on potassium (hERG, hKir2.1, hKv4.3/KChIP2.2, and hKvLQT1/hminK), calcium (hCav1.2), or sodium (hNav1.5) channels. Comparison of the IC_{50} values (i.e., >100 μ M for all channels and >300 μ M for Compound 3 in the hERG Patch Clamp assay) with C_{max} values at the 300 mg/kg dose in monkeys (approximately 48 μ M or 13,700 ng/mL) showed that adverse CV findings were noted well below the IC_{50} values.

Concentration-QTc analysis was performed on data from a double-blind, placebo-controlled FIH SAD study in healthy adult subjects. 12-lead ECGs were extracted from one time point prior to dosing and 0.25, 0.5, 1, 1.5, 2, 2.5, 3, 3.5, 4, 4.5, 6, 8, 10, 12, 14, and 24 hours post-dose on Day -1 and 1.

Compound 3 at the studied doses did not have a clinically relevant effect on heart rate or on cardiac conduction, i.e., the PR and QRS intervals. Profiles of change-from-baseline QTcF (Δ QTcF) across dose groups and post-dosing time points are shown in **Figure 6, Panel A** and corresponding plasma concentration profiles of Compound 3 and its primary metabolite are shown in **Figure 6, Panel B and C**. Mean Δ QTcF values of more than 10 msec were seen at various time points between 2 and 12 hours post-dose in the 450 to 825 mg dose groups. The largest mean Δ QTcF in the 225, 450, 750, and 825 mg group was 8.7 msec (at 6 hours post-dose), 15.1 msec (at 8 hours post-dose), 14.6 msec (at 2.5 hours post-dose) and 17.8 msec (at 10 hours post-dose), respectively. Geometric mean C_{\max} levels of Compound 3 in the 750 and 825 mg dose groups reached \sim 1190 ng/mL, whereas GM C_{\max} of the metabolite reached 86 and 97 ng/mL, respectively. Scatter plots of plasma concentrations of Compound 3 and its metabolite and Δ QTcF with linear and local regression are shown in **Figure 7, Panel A and B**.

In the C-QTc analysis, a combined model with both parent (Compound 3) and its primary metabolite as analytes was chosen as the primary model, since it had the smallest AIC value among the tested models. The goodness-of-fit plots (**Figure 7, Panel C**) demonstrate that this model provided an acceptable fit to the data. The C-QTc relationship was clearly positive with a non-significant slope of 0.00089 msec per ng/mL for Compound 3 and a statistically significant slope of 0.074 msec per ng/mL for the metabolite and a non-significant treatment specific intercept of 1.86 msec. Based on this concentration-QTc analysis, a QTc effect exceeding 10 msec can be excluded only at relatively low plasma concentrations of Compound 3 and its metabolite, \sim 551 and \sim 49 ng/mL, respectively. Predictions based on C-QTc models with each analyte separately gave comparable results.

Case study 4 - C-QTc characterization for a non-racemic therapy

Amisulpride is a dopamine D2/D3 receptor antagonist, which is approved in Europe as an orally administered atypical antipsychotic drug for treatment of acute and chronic psychosis. Amisulpride is a racemic mixture of aramisulpride and esamisulpride. Amisulpride has more recently been shown to also be an effective preventive treatment of post-operative nausea and vomiting at substantially lower IV doses²¹ and is approved for this indication in the US.

The ECG effect of amisulpride has previously been characterized in a double-blind, 4-way, single-dose, cross-over TQT study with the dose used for treatment of post-operative nausea (5 mg IV), a supratherapeutic dose (40 mg IV), placebo, and a positive control, 400 mg moxifloxacin²². Serial ECGs were recorded pre-dose and post-dose on Day 1 and at corresponding time points on Day -1. Forty healthy subjects were enrolled, of whom 17 were Japanese²². Using a linear model, the slope of the C-QTc relationship for amisulpride was 0.0169 msec (90% CI: 0.0149 to 0.019) and 0.018 msec (0.016 to 0.020) per ng/mL in White (n= 23) and Japanese (n= 17) subjects, respectively (**Figure 8, Panel A**). With these results, the QTc effect at the GM C_{\max} of 5 mg IV (169 ng/mL) and 40 mg IV (1276 ng/mL) can be predicted to 5.1 and 24.4 msec, respectively.

The effect of amisulpride alone and in combination with another commonly administered anti-emetic in the post-operative setting, ondansetron, has also been evaluated²³. In this study, 30 subjects were enrolled into a 3-way, cross-over study in which i) 10 mg IV amisulpride was given twice 2 hours apart, ii) placebo and iii) amisulpride 10 mg IV plus 4 mg IV ondansetron were given in 3 separate periods. The largest mean Δ QTcF reached 5.2 and 8.0 msec after the first and second amisulpride dose, respectively, consistent with somewhat higher GM C_{\max} levels upon repeat

administration. The largest mean $\Delta\Delta\text{QTcF}$ when amisulpride was given with ondansetron was 7.3 msec, reflecting the mild additive effect of ondansetron on the QTc interval. In the C-QTc analysis with amisulpride as the only independent variable, the slope was shallower than in the TQT study, 0.006 msec per ng/mL (90% CI: 0.002 to 0.010), with a relatively large and statistically significant intercept (2.6 msec; **Figure 8, Panel B**).

More recently, it has been shown that the enantiomers of amisulpride demonstrate stereoselective activity at the 5-HT₇ and D₂ receptors. The R-enantiomer (aramisulpride) is a more potent blocker of the 5-HT₇ receptor relative to the S-enantiomer (esamisulpride) (K_i 47 vs. 1,900 nM, respectively), whereas esamisulpride more potently inhibits the D₂ receptor (4.0 vs. 140 nM)²⁴. Based on these findings, SEP-4199, a non-racemic amisulpride in a ratio of 85:15 (aramisulpride:esamisulpride) was developed to maximize the antidepressant effect of aramisulpride via 5-HT₇ receptor antagonism, while reducing esamisulpride to minimize D₂ receptor-related extrapyramidal side effects. SEP-4199 retains some D₂ receptor-mediated activity thought to provide benefit in bipolar depression. Subsequently, the effectiveness of SEP-4199 in patients with bipolar depression was shown in a proof-of-concept study²⁵ and the program is now in late stages of development.

In non-clinical studies, both enantiomers equipotently inhibited the hERG potassium current with an IC₅₀ of 58 μM and 44 μM for aramisulpride and esamisulpride, respectively. In dog studies, QTc prolongation was observed with both enantiomers at doses above 25 to 30 mg/kg.

In a placebo-controlled randomized clinical study, the effect of a single dose of SEP-4199 was evaluated in Japanese and White healthy subjects (**Table 1**). In each dose group, 8 Japanese and 8 Caucasian subjects were enrolled, of which 6 of each race received active and 2 received placebo. Serial ECGs were extracted from continuous ECG (Holter) recordings at 3 time points prior to dosing for baseline and at 1, 2, 3, 4, 6, 8, 10, 12, and 24 hours post-dose. The effect on ΔQTcF across dose groups and time points is shown in **Figure 9, Panel A**. A clear dose-dependent effect of SEP-4199 on the QTcF interval was seen. In Panel B, a goodness-of-fit plot is shown with observed $\Delta\Delta\text{QTcF}$ across SEP-4199 plasma concentration deciles separate for each dose and the predicted effect using a linear mixed effect C-QTc model. The slope of the C-QTc relationship for SEP-4199 was similar to racemic amisulpride, 0.015 msec per ng/mL (90% CI: 0.0126 to 0.0166) with a relatively large treatment specific intercept of 6.7 msec. The goodness-of-fit plot indicates that an E_{max} model may be explored, but is unlikely to change the predicted effect on $\Delta\Delta\text{QTcF}$ at high SEP-4199 concentrations. These results are now being used to inform the dosing regimen for late-stage studies.

Case study 5 - Early development strategy for C-QTc analysis

Nezulcitinib is a novel inhaled small molecule inhibitor of the JAK pathway which is in development for the treatment of inflammation of the lungs resulting from diseases such as COVID-19 or following lung transplant.

In non-clinical assays, the IC₅₀ for nezulcitinib on the hERG channel was too high to be determined as <5% inhibition was observed at the solubility limit (13 μM), yielding a safety margin of >6500 relative to the highest observed concentration following the highest administered inhaled dose (10 mg once daily dosing [QD]) in the FIH study. In a CV study with IV administration of nezulcitinib over 4 hours that achieved concentrations exceeding 11-fold the highest observed clinical concentration, no

effect on left ventricular pressures, arterial blood pressures, heart rate or ECG intervals or waveforms was observed.

A preliminary concentration-QTc analysis was performed on data from a double-blind, placebo-controlled FIH, SAD and MAD study in healthy adult subjects (NCT04350736; **Table 1**). Nezulcitinib was given by inhalation via the PARI eFlow nebulizer system. For this analysis, 12-lead safety ECGs recorded prior to dosing and 4, 8 and 24 hours post-dose on Day 1 in both the SAD and MAD and on Day 7 in the MAD were used²⁶. PK samples were collected at 0.5, 1, 2, 4, 6, 7, 12, and 24 hours post-dose on Day 1 and at pre-dose, 2, 4, 6, 7, 12, and 24 hours on Day 7. Continuous ECG (Holter) recordings were collected and stored, with serial ECGs to be extracted at the PK time points when proof-of-concept was demonstrated in a future study.

Nezulcitinib at the studied doses did not have a clinically relevant effect on heart rate. Profiles of Δ QTcF from the safety ECGs and nezulcitinib plasma concentration across dose groups and post-dosing time points are shown in **Figure 10, Panel A and B**. In general, the smallest mean Δ QTcF was seen in the highest dose group (10 mg) and there is no indication of a dose-dependent effect. Nezulcitinib accumulation in the plasma was minimal (accumulation ratio of 1.1 for AUC and 1.0 for C_{max}) following QD dosing for 7 days. The pattern of mean Δ QTcF across active dose groups and placebo suggests that nezulcitinib does not exert a meaningful effect on the QTc interval. Although the safety ECG data utilized in this analysis was not collected at the time of expected C_{max} (1 hour postdose), the studied concentration range (up to 42.2 ng/mL) exceeded mean $C_{max,ss}$ (17.6 ng/mL) for a clinical dose of 3 mg QD.

Nezulcitinib plasma concentrations were pooled from the SAD and MAD portion of the study based on the limited accumulation with repeated dosing, plotted against Δ QTcF and fitted using linear and local regression in Figure 11, Panel A. There was little divergence between a simple linear regression and the LOESS, which indicated that a linear C-QTc model may be appropriate.

A linear mixed-effects model with a treatment specific intercept provided an acceptable fit to the observed QTcF data and was used to establish the relationship between plasma concentrations of nezulcitinib and Δ QTcF (**Figure 11, Panel B**). No relationship was observed in the C-QTc relationship with a slope of -0.0425 msec per ng/mL (90% CI: -0.427 to 0.345) and a small, non-significant treatment specific intercept of -0.21 msec. Based on limited data from the safety ECGs, an effect on Δ QTcF exceeding 10 msec can be excluded within the full range of observed nezulcitinib plasma concentrations up to ~30 ng/mL, which exceeded the observed mean $C_{max,ss}$ at the clinical dose of 3 mg (17.6 ng/mL in the MAD study). A definitive analysis using 12-lead ECGs extracted from the collected and stored continuous (Holter) recordings paired with data from the full PK profile is expected to confirm the effect at the '*High Clinical Exposure scenario*' once the efficacy of nezulcitinib has been demonstrated in Phase 2 clinical trials.

Discussion

To ensure the immediate safety of participating subjects, 12-lead safety ECGs, in most cases evaluated on-site by the investigator, remain an important part of FIH trials. With the R(3) revision of ICH E14 from 2015², FIH studies can now also be used to conclusively exclude that a new drug has a clinically concerning effect on ECG parameters, including the QTc interval.

When using a study without a positive control (e.g., a FIH SAD or MAD study) to provide conclusive evidence of the absence of a clinically relevant effect on QTc (i.e., an effect < 10 msec), and thereby replacing the TQT study, some key elements have to be met²:

There are data characterizing the response at a sufficiently high multiple of the clinically relevant exposure [see Question 5.1 in ICH E14 Q&A (R3)]².

Based on regulatory precedents, a 2-fold margin between achieved levels in the SAD/MAD study and the *High clinical exposure* is often deemed sufficient. FDA's definition of *High clinical exposure* is now detailed in the recently endorsed S7B/E14 Q&A document^{27,28}: '*High clinical exposure: exposure (C_{max,ss}) achieved when the maximum therapeutic dose is administered in the presence of the intrinsic or extrinsic factor (e.g. organ impairment, drug-drug interaction, food effect, etc.) that has the largest effect on increasing C_{max,ss}*'. When sufficiently high concentrations cannot be achieved due to e.g., safety, tolerability, or saturating absorption), the ongoing revision, however, opens another option²⁷: '*...a nonclinical integrated risk assessment can be used as supplementary evidence.; in summary, the nonclinical studies should include (1) (1) a hERG assay, following best practice considerations (see ICH S7B Q&A 2), that shows low risk as defined in ICH S7B Q&As 1.1-1.2 and (2) no evidence of QTc prolongation in an in vivo assay conducted according to ICH S7B at exposures that cover high clinical exposures (see ICH S7B Q&As 1.1 and 3;....*²⁷

Based on the 2015 E14 revision, there is a clear trend of decreasing number of TQT studies. Among all studies submitted to FDA between 2016 and August 2020 for the purpose of providing a definitive evaluation of ECG effects (on average 55/year), the proportion of TQT studies has decreased from 62% to 34%, and the proportion of FIH SAD/MAD studies (so-called 5.1 studies) has increased from 10% to 42%, while QT evaluation applied in oncology studies has been relatively constant, around 26-27%²⁷. Numbers for 2021 are similar, with 35% TQT studies and 38% 5.1 studies. With the now finalized S7B/E14 Q&A document (February 2022)²⁸, it can be expected that this trend will further continue.

In this publication, we share 5 examples of SAD and/or MAD studies from different sponsors that illustrate different strategies for conclusive ECG evaluation in early clinical studies, all with the objective of obviating the TQT study later in development. In all examples, serial ECG monitoring was implemented and procedures for collection of digital ECG data were described in the protocol. This allows the sponsor to collect and store the ECG data and make a decision if and when to analyze, based on observed PK in patients and also on other project considerations, such as having met proof-of-efficacy. The protocol must specify that ECGs are to be recorded/collected after supine rest at time points paired with PK sampling. Using the approach of collecting and storing ECG data constitutes an efficient way from a resource perspective to address the regulatory need of

conclusively excluding small effects on ECG parameters. It also allows the sponsor to tailor the timing and costs of the ECG analysis to the needs of the project.

Case 1 represents an example in which data were analyzed at a stage when the PK profile was fully characterized in the target patient population, and it seems very likely that a TQT study will be waived. Case 2, on the other hand, is an example when the sponsor saw the need to exclude drug-induced ECG effects and it remains open as to whether drug concentrations achieved in the SAD study will be high enough to replace the TQT study. If mean C_{max} exceeds the *High clinical exposure*, but not with sufficient margin, the option of conducting complementary non-clinical assays as described in the S7B/E14 Q&A document remains. If these are undertaken, the goal of replacing the TQT study may still be achievable with an integrated non-clinical/clinical risk assessment²⁸. An alternative would be to conduct a study with higher doses in healthy subjects and pool data with the FIH study, with the caveats mentioned above in terms of pooling when performing C-QTc analysis. When considering the timing of the C-QTc analysis of FIH data, it should be pointed out that in order to allow for routine ECG monitoring in line with clinical practice of the therapeutic area, conclusive evidence of the absence of relevant ECG effects should be available before initiating Phase 3 studies. Besides this, many internal considerations will affect the timing of the ECG analysis, such as prioritization across programs, partnering discussions and unmet medical need. Case 5 represents an alternative of collecting and storing, as compared to Case 1 and 2. The example is based on a SAD FIH study with an inhaled compound for which the highest possible dose that can be practically administered will also to be evaluated in patients. The sponsor viewed it as important to get a 'first read' on any potential ECG effects, before proceeding to proof-of-efficacy in patients. Safety ECGs with intervals measured by the ECG machine were therefore used in a preliminary C-QTc analysis with ECG matched to the nearest measured drug plasma concentration. Results of this analysis were clearly negative, i.e., an effect on $\Delta\Delta QTc$ exceeding 10 msec could be excluded across the range of observed plasma concentrations. The results led to the decision to proceed to proof-of-efficacy with the program, with the intention that the definitive C-QT analysis would be conducted using ECG data extracted from the stored Holter recordings from all time points where PK samples were collected. This exploratory analysis using a limited number of PK-ECG pairs provided confidence for the Sponsor to engage regulatory agencies early in the drug development process to agree that the results of a definitive C-QTc analysis, the hERG assay data and dog CV study results would provide a favorable integrated non-clinical/clinical risk assessment and therefore waive the need for a full TQT study. This early analysis helped clarify the CV safety development pathway for nezulcitinib, while optimizing resources by postponing the definitive C-QTc analysis of Holter extracted, high quality ECGs and submission of a TQT study waiver until after the completion of a Phase 2 efficacy/safety trial.

Case 3 is SAD FIH study in which an effect on the QTc interval exceeding 10 msec could not be excluded, despite non-clinical assays, which were deemed negative at clinically relevant plasma concentration levels. The sponsor decided to implement procedures and to analyze obtained ECG data from the FIH SAD study early in the program, which helped making an informed decision on subsequent development. Concentration – QTc analysis applied to the data from the FIH SAD study indicated a dose dependent effect on QT interval with >10 msec $\Delta\Delta QTcF$ at an exposure close to the anticipated efficacious human exposure. The observed QTcF effect was not predicted by nonclinical assays/studies. The hERG assay, as well as selected ion channels inhibition assays, were negative for

both Compound 3 and its primary metabolite. In toxicology studies in non-human primates, increases in ECG interval parameters and alterations in waveform morphology were observed at high doses with high safety margin as compared to the anticipated efficacious human exposure. The QTc effect observed in the FIH SAD study, along with overall benefit-risk assessment, supported the decision of postponing the MAD study and the subsequent clinical development program.

Amisulpride has a well characterized QTc effect, based on a previously conducted, published TQT study. Amisulpride is a racemic mixture and the sponsor is now developing SEP-4199, non-racemic amisulpride in a ratio of 85:15 (aramisulpride:esamisulpride) for the treatment of bipolar depression, based on stereoselective activity at the 5-HT₇ and D₂ receptors. The relative contribution of each enantiomer on the QTc effect was not known. A dose finding study in Japanese and White subjects was therefore conducted to evaluate the QTc effect on SEP-4199 and to optimize the dosing regimen in patient studies. The C-QTc analysis demonstrated a slope of the relationship close to the one observed in the TQT study (0.015 vs. 0.017 msec per ng/mL) and thereby confirmed the observations in non-clinical assays, with equipotent hERG inhibition and QTc prolongation in dogs at high doses.

In 4 of the 5 examples, the basic linear model described in the white paper on C-QTc analysis¹⁰ was used and turned out to be appropriate for the purpose of assessing the potential effect of the drug on the QTc interval. In case 3, both parent and metabolite seem to contribute to the observed effect. In such a case, both analytes need to be considered for modelling in order to exclude hysteresis. It should, however, be noted that in this case, all 3 models (parent alone, metabolite alone and both analytes) came to similar conclusions. The set of graphic presentations given here are usually a good basis to judge the appropriateness of the model. The quantile plots demonstrate that the model fit is reasonable and the treatment specific intercept is small.

The width of the confidence interval, graphically displayed in the goodness-of-fit plot, is a useful indicator of the power of the study to exclude an effect on the QTc interval. Standard power calculations for studies based on concentration-effect models are not straightforward, as the standard error of a prediction is dependent on many details of the data and the model used. Simulations based on moxifloxacin data from more than 100 TQT studies performed by Huang et al have shown that a study with 24 subjects will in most cases provide sufficient power to demonstrate assay sensitivity based on a C-QTc model²⁹. This however applies to TQT studies in which the number of subjects on a high dose are higher than FIH dose-escalation studies. Simulations performed by Ferber et al³⁰ have also shown that including a sufficient number of subjects on placebo is important to control the number of false negative studies. The sample size of FIH studies is not typically based on a formal power calculation to exclude ECG effects. However, studies with 4 to 5 dose groups of 8 subjects per group (6 active and 2 placebo) are typically considered sufficient to enable the exclusion of a 10 msec effect at therapeutic concentrations for drugs with a small underlying 'true' effect (e.g., ≤ 3 msec).

The scatter plot of observed Δ QTc and concentrations with simple linear and local regression and the quantile plots can serve as a starting point for a more refined modelling. As an example, in Case 4, a nonlinear model, e.g., an E_{\max} model, may provide a better fit to the data and thereby improved the prediction of the QTc effect. In most cases, this is not required by regulators (see White Paper¹⁰), but it can be helpful for further internal decisions. The models fitted for example 3 can also serve as a starting point to investigate the role of parent and metabolite in the effect on QTc seen.

None of the examples discussed in this publication addresses the scenario when a drug, such as many of those intended to treat cancer, cannot be safely given in high doses to healthy subjects. In such case, the standard has been to apply as many of the elements as possible from the TQT study into trials in the targeted patient population. In many studies in cancer patients, the highest tolerable dose is given and there is no placebo treatment and no positive control. Within the inherent limitations of this design, C-QTc analysis can also be applied to demonstrate the lack of a concerning effect on the QTc interval, provided PK is collected, e.g., in the dose-escalation phase of a FIH study in cancer patients³¹. Such studies are referred to as 6.1 studies in the recently endorsed S7B/E14 Q&A document, which will further promote the utility for this purpose of early patient trials for drugs that cannot be safely given in high doses to healthy subjects^{27,28}.

Conclusions

Based on the 2015 revision of the ICH E14 guidance², the number of development programs in which the TQT study has been successfully replaced by C-QTc analysis applied to FIH ECG/PK data is steadily increasing. The recently endorsed S7B/E14 Q&A document (February 2022) will, to some extent, further strengthen this trend by allowing an integrated non-clinical/clinical risk assessment, provided standardized non-clinical assays are used or added²⁷.

Tables

Table 1: Key design features of included case studies

Case Study	NCE Route	Design	# Dose groups/ active/ placebo	Dose range, mg	Baseline	Serial ECGs
1.	E2027 Oral	SAD	11/71/2 1	10 to 1200	Day -1	Day -1 and 1
		MAD QD	5/30/10	25 to 400	Day -1	Day -1, 1 and 14
2.	Compound 2 Oral	SAD	8/50/16	3 to 200	Day 1 pre-dose	Day 1
3.	Compound 3 Oral	SAD	6/42/13	25 to 825	Day -1	Day -1 and 1
4.	SEP-4199 Oral	SAD	6/48/12	200 to 700	Day 1 pre-dose	Day 1
5.	Nezulcitinib Inhaled	SAD	3/18/6	1 to 10	Day 1 pre-dose	Day 1
		MAD QD	3/24/6	1 to 10	Day 1 pre-dose	Day 1 and 7

Abbreviations: Active/placebo: Total number of subjects on active and on placebo, pooled across dose groups; *SAD:* Single ascending dose study; *MAD:* Multiple ascending dose study; *NCE:* New chemical entity; *Route:* Route of administration; *QD:* Once daily

Figure legends

Figure legends

Figure 1: Lemborexant concentration-QTc analysis on data from 2 MAD studies

Goodness-of-fit plot for observed QTc values and predicted relation between lemborexant plasma levels and $\Delta\Delta\text{QTcI}$ on pooled data from a FIH MAD study and a Japanese bridging MAD study. Red squares with vertical bars denote the observed mean $\Delta\Delta\text{QTcI}$ with 90%CI displayed at the median plasma concentration within each decile. The solid black line with gray-shaded area denotes the C-QTc model-predicted mean $\Delta\Delta\text{QTcI}$ with 90% CI. The horizontal red lines with notches show the range of plasma concentrations divided into deciles.

Figure 3B in Murphy et al⁹. Reproduced with permission from the authors.

Figure 2: E2027

Panel A: SAD - Change-from-baseline QTcF (ΔQTcF) across dose groups and time points

The pattern of ΔQTcF across dose groups, including the pooled placebo group, does not suggest that single doses of E2027 prolongs the QTc interval in a dose-dependent way.

Mean \pm 90% CI ΔQTcF across post-dose time points.

Panel B: SAD – E2027 plasma concentration profile across dose groups

The highest concentrations were observed between 2 and 4 hours post-dose in the highest dose groups (400, 800 and 1200 mg). Mean concentrations were higher in the E2027 800 mg dose group than in the 1200 mg group, probably due to limited absorption and variability within small dose groups.

Mean \pm 90% CI, calculated from descriptive statistics

Panel C: MAD - Change-from-baseline QTcF (ΔQTcF) across dose groups and time points

Mean \pm 90% CI ΔQTcF across post-dose time points.

Panel D: MAD - Plasma concentration profile across dose groups

Substantial accumulation was observed with multiple dosing. E2027 concentrations on Day 14 were similar between Japanese and non-Japanese subjects in the 400 mg groups.

Mean \pm 90% CI, calculated from descriptive statistics

Figure 3: E2027

Panel A: Scatter plot on data from both SAD and MAD.

The blue squares and red filled circles denote the pairs of observed E2027 plasma concentrations and $\Delta\Delta\text{QTcF}$ (derived from the individual ΔQTcF for the active subtracted by the mean predicted ΔQTcF for placebo from the model) for the non-Japanese (blue) and Japanese (red) subjects, respectively. The black solid and dashed lines denote the model-predicted mean $\Delta\Delta\text{QTcF}$ with 90% CI.

Panel B: Goodness-of-fit plot

Goodness-of-fit plot for observed $\Delta\Delta\text{QTc}$ and predicted $\Delta\Delta\text{QTcF}$ on pooled data from the E2027 FIH SAD and MAD study in Japanese and non-Japanese healthy subjects. Red squares with vertical bars denote the observed mean $\Delta\Delta\text{QTcF}$ with 90%CI displayed at the median plasma concentration within each decile. The solid black line with gray-shaded area denotes the C-QTc model-predicted mean $\Delta\Delta\text{QTcF}$ with 90% CI. The horizontal red lines with notches show the range of E2027 plasma concentrations divided into deciles.

Figure 4: Compound 2

Panel A: Change-from-baseline QTcF (ΔQTcF) across dose groups and time points

Mean \pm 90% CI ΔQTcF across post-dose time points.

Panel B: Plasma concentration profile across dose groups

Mean \pm 90% CI calculated from descriptive statistics.

Figure 5: Compound 2

Panel A: Scatter plot with linear and local regression

The red line with the blue shaded area denotes the LOESS regression and 90% CI. The black solid line denotes the simple linear regression line. The plotted points denote the pairs of observed Compound 2 plasma concentrations and ΔQTcF . The linear regression line falls within the 90% CI of LOESS in most of the concentration range, thereby illustrating that a linear model captures the data across the concentration range in an acceptable way.

Panel B: Goodness-of-fit plot

Goodness-of-fit plot for observed $\Delta\Delta\text{QTcF}$ and predicted $\Delta\Delta\text{QTcF}$ on data from the Compound 2 FIH SAD study in healthy subjects. Red circles with vertical bars denote the observed mean $\Delta\Delta\text{QTcF}$ with 90% CI displayed at the median plasma concentration within each concentration decile for Compound 2. The solid black line with gray shaded area denotes the model-predicted mean $\Delta\Delta\text{QTcF}$ with 90% CI. The horizontal red line with notches shows the range of concentrations divided into deciles for Compound 2.

Figure 6: Compound 3

Panel A: Change-from-baseline QTcF (ΔQTcF) across dose groups and time points

Mean \pm 90% CI ΔQTcF across post-dose time points.

Panel B: Compound 3 plasma concentration profile across dose groups

Mean \pm SD calculated from descriptive statistics.

Panel C: Metabolite plasma concentration profile across dose groups

Mean \pm SD calculated from descriptive statistics.

Figure 7: Compound 3

Panel A: Scatter plot with linear and local regression, parent drug

The plotted points denote the pairs of observed Compound 3 plasma concentrations and ΔQTcF . The red line with the blue shaded area denotes the LOESS regression and 90% CI. The black solid line denotes the simple linear regression line. It can be seen that the linear regression captures the data across the concentration range in an acceptable way.

Panel B: Scatter plot with linear and local regression, metabolite

The linear regression line falls outside and above the LOESS 90% CI, suggesting that simple linear regression may overestimate the effect on $\Delta\Delta\text{QTc}$ at higher concentration levels.

Panel C: Goodness-of-fit plot

Goodness-of-fit plot for observed $\Delta\Delta\text{QTcF}$ and predicted $\Delta\Delta\text{QTcF}$ on data with the metabolite from the Compound 3 FIH SAD study in healthy subjects. It seems that the model to some extent underestimates the observed data at high concentrations.

Symbols as in Figure 5.

Figure 8: Amisulpride

Panel A: Concentration- QTc relationship in a TQT study with amisulpride

Scatter plot of $\Delta\Delta\text{QTcF}$ against the amisulpride plasma concentration (ng/ml). Regression lines for amisulpride derived from a linear mixed effect model. The 90% CIs are represented by grey shading for the slope in Japanese subjects and red shading for the slope in White subjects.

Figure 3B in Taubel et al. British J Clin Pharm 2017; 83: 338-49²² With permission from the publisher, John Wiley and Sons inc.

Panel B: Concentration- QTc relationship in a study with amisulpride alone and in combination with ondansetron

Scatter plot of observed amisulpride plasma concentrations and $\Delta\Delta\text{QTcF}$ by subject. The solid red line with dashed red lines denotes the model-predicted mean $\Delta\Delta\text{QTcF}$ with 90% CI using a model with amisulpride as the only analyte. The blue squares and red triangles denote the pairs of observed amisulpride plasma concentrations and $\Delta\Delta\text{QTcF}$ by subjects for the amisulpride and amisulpride + ondansetron treatment periods, respectively.

Figure 4A in Fox et al. Anesth Analg 2021; 132: 150-159²³

Figure 9: SEP-4199

Panel A: Change-from-baseline QTcF (ΔQTcF) across dose groups and time points

Mean \pm 90% CI ΔQTcF across post-dose time points.

Panel B: Goodness-of-fit plot

Goodness-of-fit plot for observed $\Delta\Delta\text{QTcF}$ and predicted $\Delta\Delta\text{QTcF}$ on data from a SAD study in healthy subjects with SEP-4199. The model seems to slightly underestimate the effect on $\Delta\Delta\text{QTcF}$ at high concentrations.

Symbols as in Figure 5.

Figure 10: Nezulcitinib

Panel A: Placebo-corrected change-from-baseline QTcF across dose groups and time points

Data from safety ECGs and the matched, nearest concentration value in the SAD and MAD cohorts.

Mean \pm 90% CI Δ QTcF across post-dose time points.

Panel B: Plasma concentration profile across dose groups in the SAD and MAD cohorts

Mean \pm standard deviation Δ QTcF across post-dose time points.

Figure 11: Nezulcitinib

Panel A: Scatter plot with linear and local regression

The red line with the light grey shaded area denotes the LOESS regression and 90% CI. The black solid line denotes the simple linear regression line. The plotted points denote the pairs of observed nezulcitinib plasma concentrations and Δ QTcF pooled from the SAD and MAD portion of the study.

Panel B: Goodness-of-fit plot

Goodness-of-fit plot for observed $\Delta\Delta$ QTcF and predicted $\Delta\Delta$ QTcF on data from a SAD study in healthy subjects with nezulcitinib.

Symbols as in Figure 5.

Data sharing

Data access may be requested from individual co-authors.

References

1. ICH E14 The Clinical Evaluation of QT/QTc Interval Prolongation and Proarrhythmic Potential for Non-Antiarrhythmic Drugs. Available at: http://www.ich.org/fileadmin/Public_Web_Site/ICH_Products/Guidelines/Efficacy/E14/E14_Guideline.pdf, 2005
2. ICH E14 Questions & Answers (R3) December 10, 2015. Available at: http://www.ich.org/fileadmin/Public_Web_Site/ICH_Products/Guidelines/Efficacy/E14/E14_Q_As_R3__Step4.pdf, 2015
3. Darpo B, Garnett C. Early QT assessment--how can our confidence in the data be improved? *Br J Clin Pharmacol*. 2013; 76: 642-648.
4. Garnett C, Beasley N, Bhattaram VA, et al. Concentration-QT relationships play a key role in the evaluation of proarrhythmic risk during regulatory review. *J Clin. Pharmacol*. 2008; 48: 13-18.
5. Darpo B, Benson C, Dota C, et al. Results from the IQ-CSRC prospective study support replacement of the thorough QT study by QT assessment in the early clinical phase. *Clin Pharmacol Ther*. 2015; 97: 326-335.
6. Darpo B, Garnett C, Keirns J, et al. Implications of the IQ-CSRC Prospective Study: Time to Revise ICH E14. *Drug Saf*. 2015; 38: 773-780.
7. Darpo B, Sarapa N, Garnett C, et al. The IQ-CSRC prospective clinical Phase 1 study: "Can early QT assessment using exposure response analysis replace the thorough QT study?". *Ann. Noninvasive Electrocardiol*. 2014; 19: 70-81.
8. Nelson CH, Wang L, Fang L, et al. A Quantitative Framework to Evaluate Proarrhythmic Risk in a First-in-Human Study to Support Waiver of a Thorough QT Study. *Clin Pharmacol Ther*. 2015; 98: 630-638.
9. Murphy PJ, Yasuda S, Nakai K, et al. Concentration-Response Modeling of ECG Data From Early-Phase Clinical Studies as an Alternative Clinical and Regulatory Approach to Assessing QT Risk - Experience From the Development Program of Lemborexant. *J Clin Pharmacol*. 2017; 57: 96-104.
10. Garnett C, Bonate PL, Dang Q, et al. Scientific white paper on concentration-QTc modeling. *J Pharmacokinet Pharmacodyn*. 2018; 45: 383-397.
11. Hurvich CS, JS; Tsai, CL. Smoothing parameter selection in nonparametric regression using an improved Akaike Information Criterion. *J R Stat Soc Series B Stat Methodol*. 1998; 60: 271-293.
12. Ferber G: Issues with exposure-response analysis: How we close the gap. Presentation on "New Advances in the Assessment of Drug-Induced Arrhythmias and the Comprehensive In Vitro Proarrhythmia Assay (CiPA). Cardiac Safety Research Consortium (CSRC) HESI meeting. May 21-22, 2018
13. Kenward MG, Roger JH. Small sample inference for fixed effects from restricted maximum likelihood. *Biometrics*. 1997; 53: 983-997.
14. Dang Q, Zhang J. Validation of QT Interval Correction Methods When a Drug Changes Heart Rate. *Ther Innov Regul Sci*. 2013; 47: 256-260.
15. Garnett C, Zhu H, Malik M, et al. Methodologies to characterize the QT/corrected QT interval in the presence of drug-induced heart rate changes or other autonomic effects. *Am. Heart J*. 2012; 163: 912-930.
16. Soave D, Sun L. A generalized Levene's scale test for variance heterogeneity in the presence of sample correlation and group uncertainty. *Biometrics*. 2017; 73: 960-971.
17. Tornoe CW, Garnett CE, Wang Y, et al. Creation of a knowledge management system for QT analyses. *J. Clin. Pharmacol*. 2011; 51: 1035-1042.

18. Hershey LA, Coleman-Jackson R. Pharmacological Management of Dementia with Lewy Bodies. *Drugs Aging*. 2019; 36: 309-319.
19. van der Linde HJ, Van Deuren B, Teisman A, et al. The effect of changes in core body temperature on the QT interval in beagle dogs: a previously ignored phenomenon, with a method for correction. *Br J Pharmacol*. 2008; 154: 1474-81.
20. Cleveland W. Robust locally weighted regression and smoothing scatterplots. *J Am Stat Assoc*. 1979; 74: 829-836.
21. Kranke P, Bergese SD, Minkowitz HS, et al. Amisulpride Prevents Postoperative Nausea and Vomiting in Patients at High Risk: A Randomized, Double-blind, Placebo-controlled Trial. *Anesthesiology*. 2018; 128: 1099-1106.
22. Taubel J, Ferber G, Fox G, et al. Thorough QT study of the effect of intravenous amisulpride on QTc interval in Caucasian and Japanese healthy subjects. *Br J Clin Pharmacol*. 2017; 83: 339-348.
23. Fox GM, Albayaty M, Walker JL, et al. Intravenous Amisulpride Does Not Meaningfully Prolong the QTc Interval at Doses Effective for the Management of Postoperative Nausea and Vomiting. *Anesth Analg*. 2019;
24. Hopkins SC, Wilkinson S, Corriveau TJ, et al. Discovery of Nonracemic Amisulpride to Maximize Benefit/Risk of 5-HT₇ and D₂ Receptor Antagonism for the Treatment of Mood Disorders. *Clin Pharmacol Ther*. 2021; 110: 808-815.
25. Loebel A, Koblan KS, Tsai J, et al. A Randomized, Double-blind, Placebo-controlled Proof-of-Concept Trial to Evaluate the Efficacy and Safety of Non-racemic Amisulpride (SEP-4199) for the Treatment of Bipolar I Depression. *J Affect Disord*. 2021; 296: 549-558.
26. Pfeifer ND, Lo A, Bourdet DL, et al. Phase I study in healthy participants to evaluate safety, tolerability, and pharmacokinetics of inhaled nezulcitinib, a potential treatment for COVID-19. *Clin Transl Sci*. 2021;
27. Darpo B, Ferber G. The New S7B/E14 Question and Answer Draft Guidance for Industry: Contents and Commentary. *J Clin Pharmacol*. 2021; 61: 1261-1273.
28. S7B/E14 Q&A February 2022. Clinical and Nonclinical Evaluation of QT/QTc Interval Prolongation and Proarrhythmic Potential. Questions and Answers. Available at: <https://ich.org/page/safety-guidelines>.
29. Huang DP, Chen J, Dang Q, et al. Assay sensitivity in "Hybrid thorough QT/QTc (TQT)" study. *J Biopharm Stat*. 2019; 29: 378-384.
30. Ferber G, Sun Y, Darpo B, et al. Study Design Parameters Affecting Exposure Response Analysis of QT Data: Results From Simulation Studies. *J Clin Pharmacol*. 2018;
31. Ogasawara K, Xu C, Yin J, et al. Evaluation of the Potential for QTc Prolongation With Repeated Oral Doses of Fedratinib in Patients With Advanced Solid Tumors. *Clin Pharmacol Drug Dev*. 2020; doi: 10.1002/cpdd.850. Online ahead of print.

Figures

Figure 1

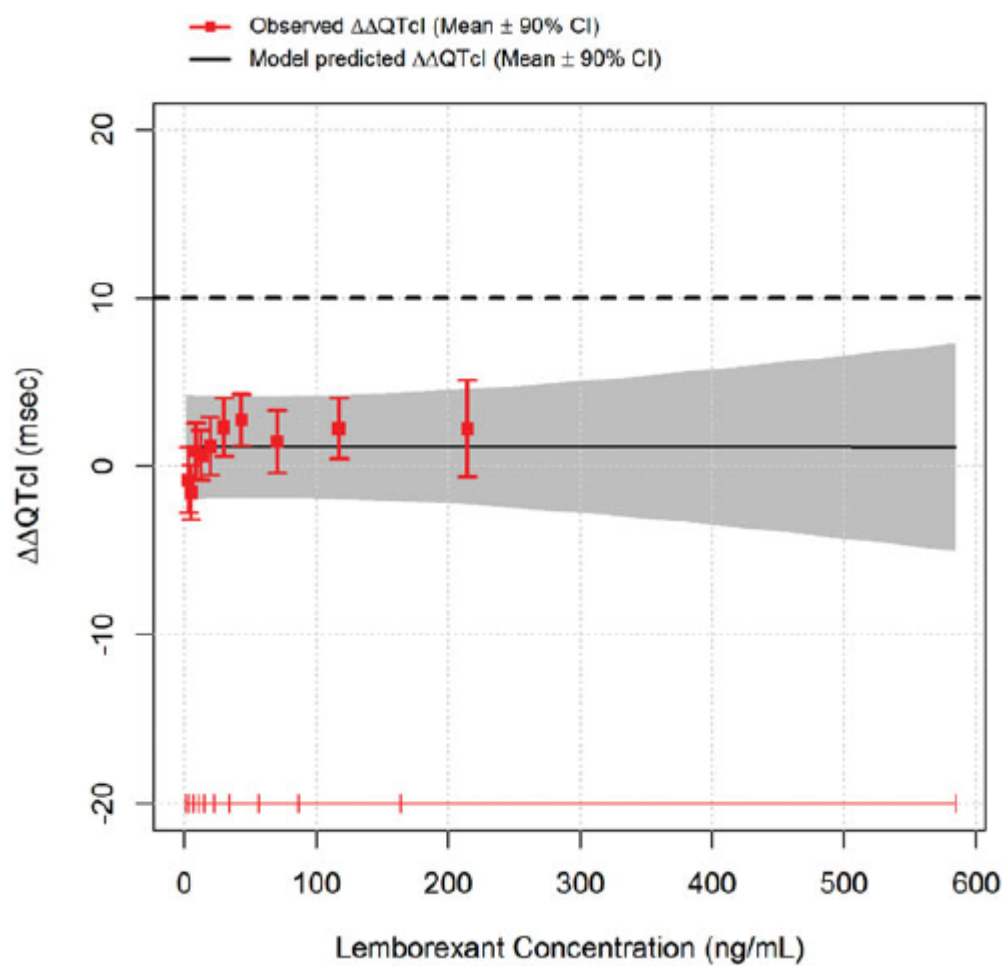
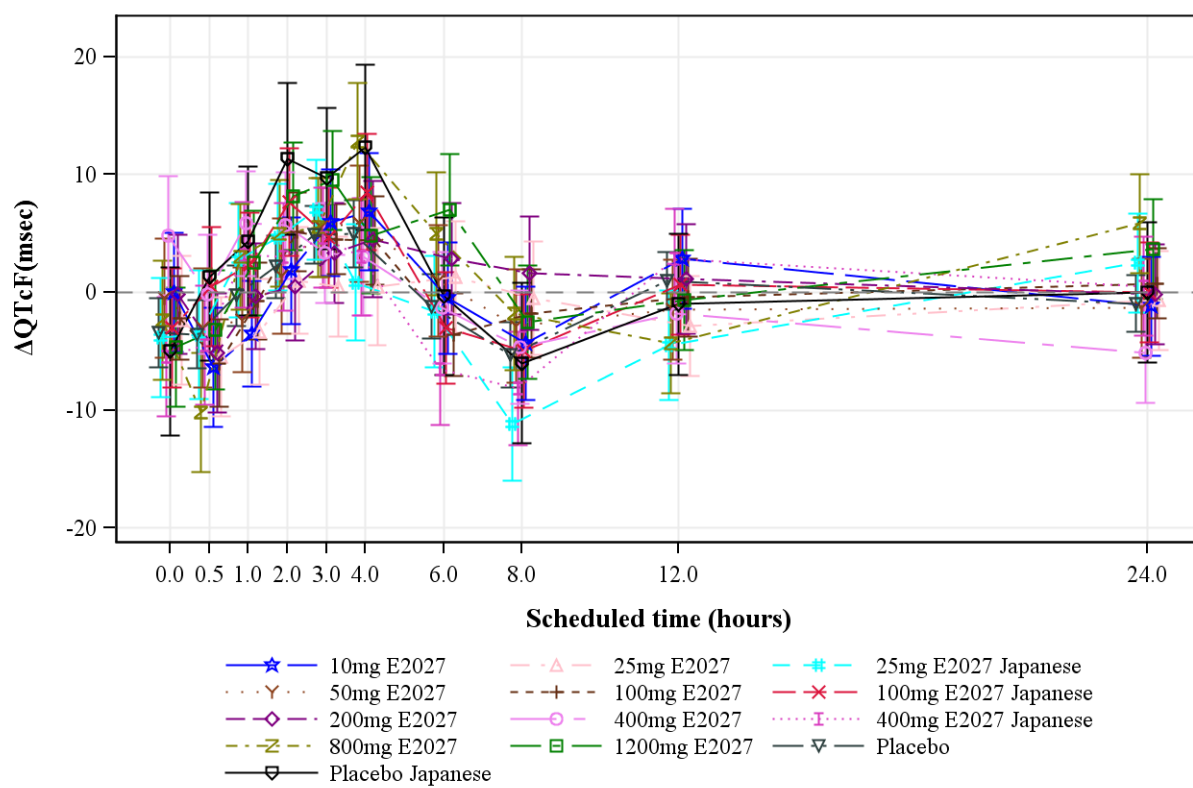
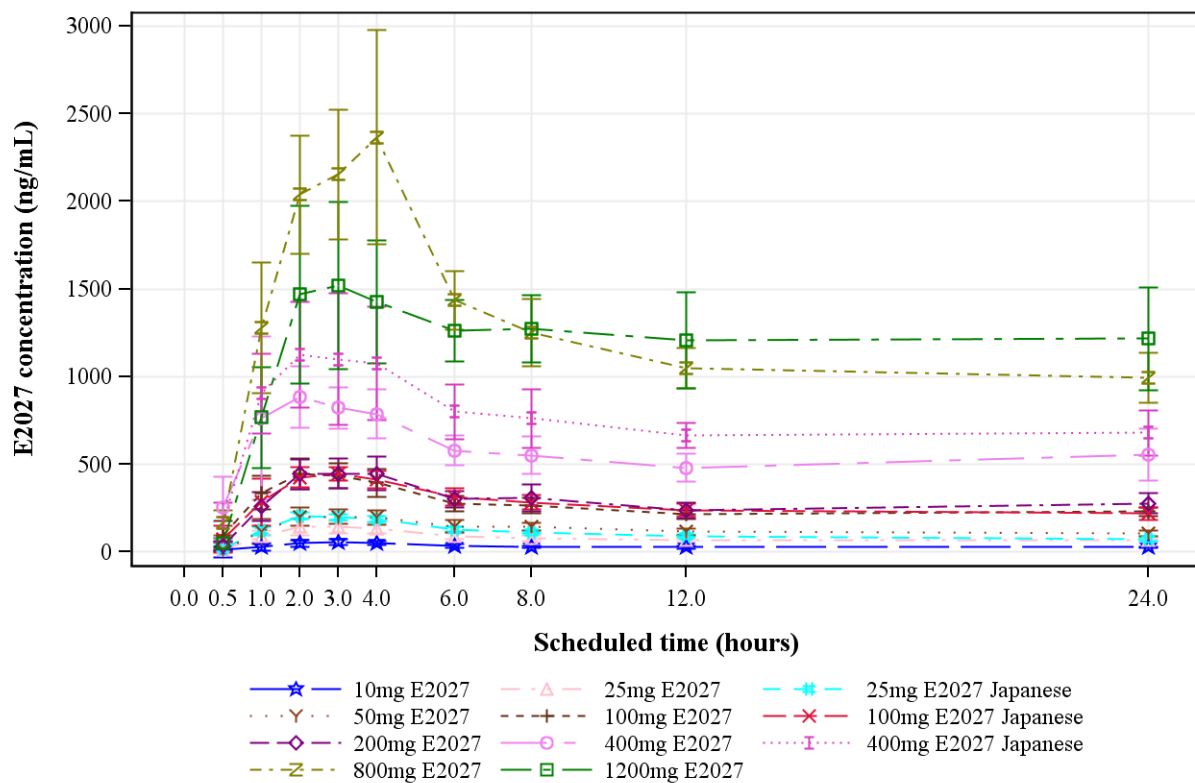


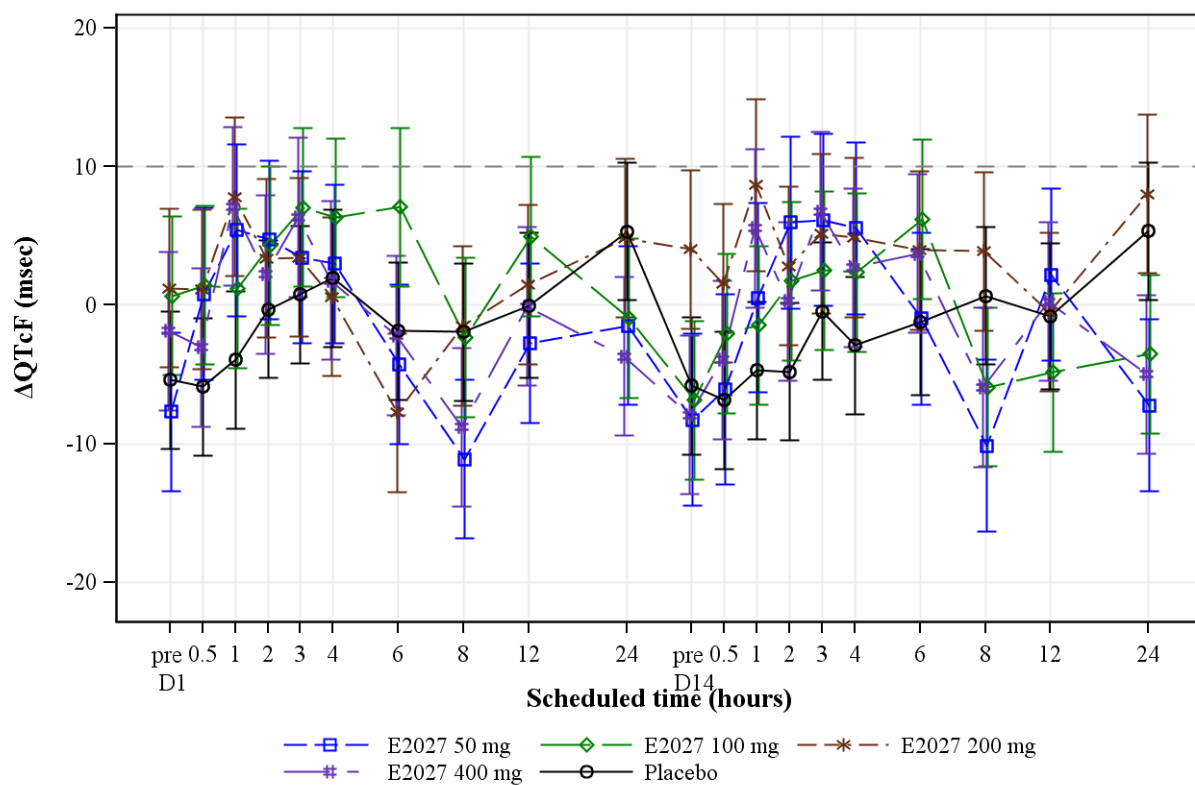
Figure 2
Panel A



Panel B



Panel C



Panel D

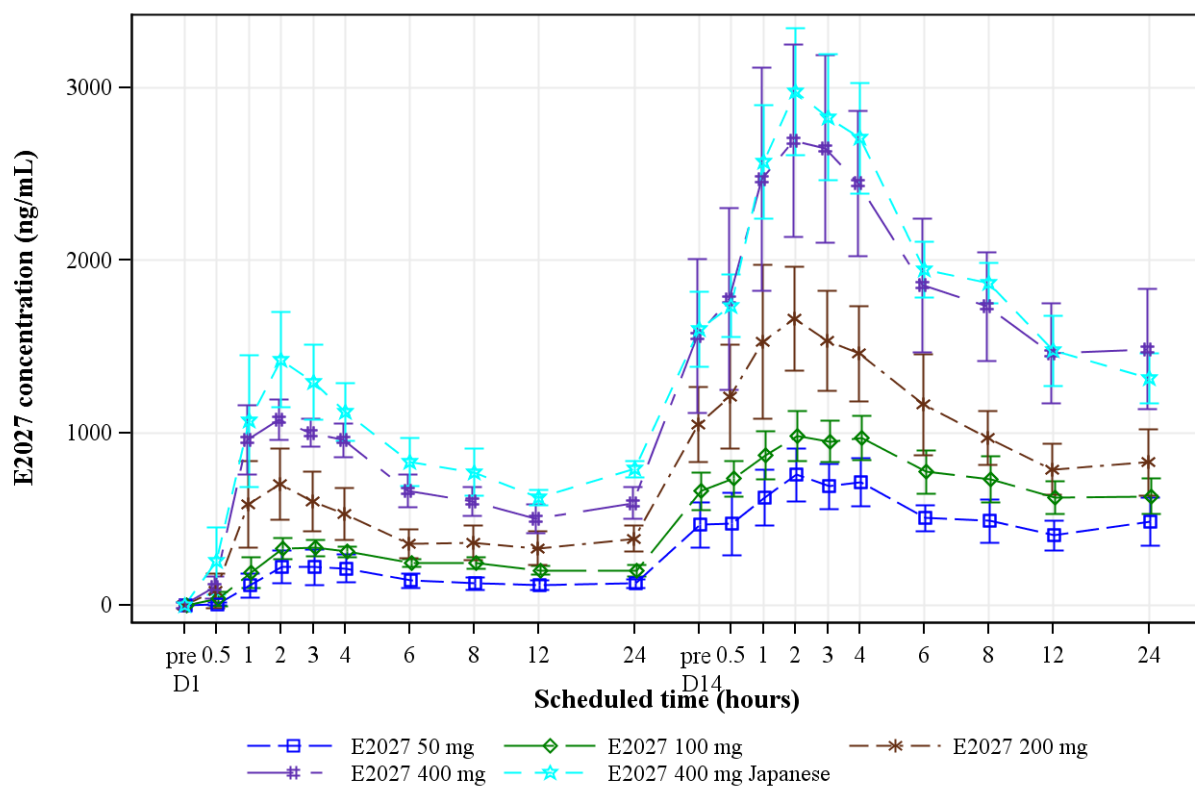
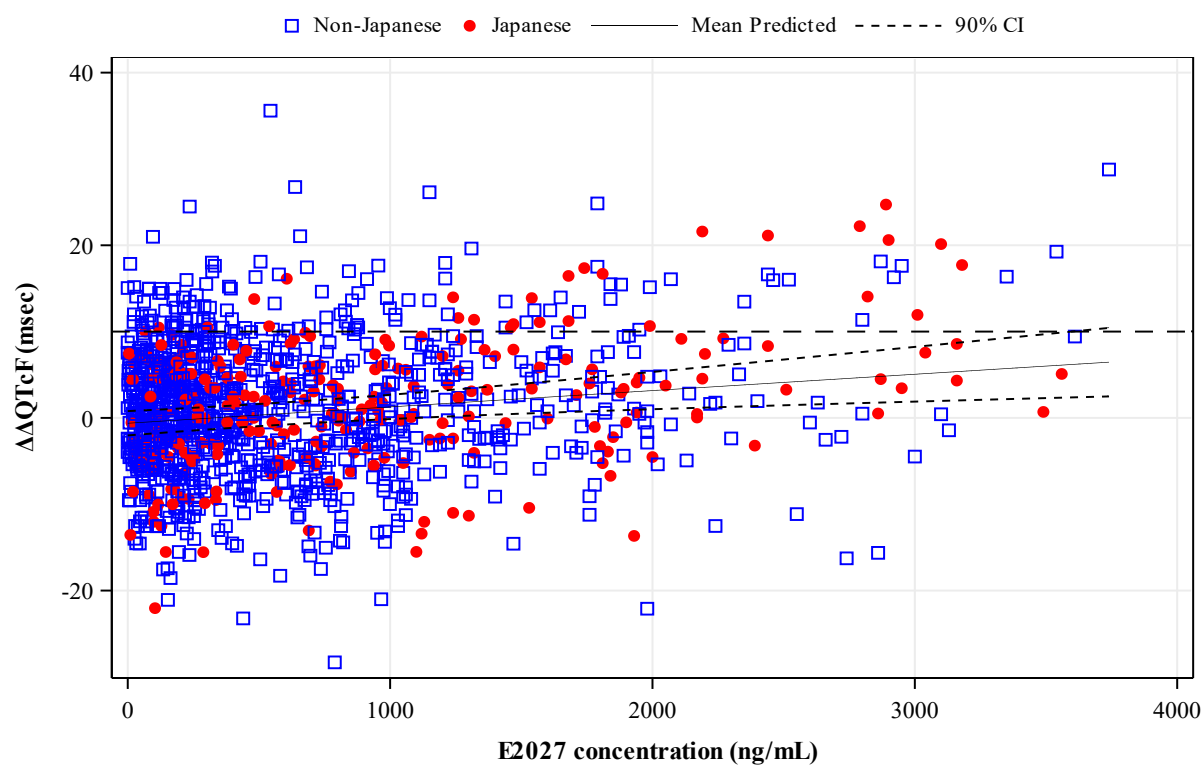


Figure 3
Panel A



Panel B

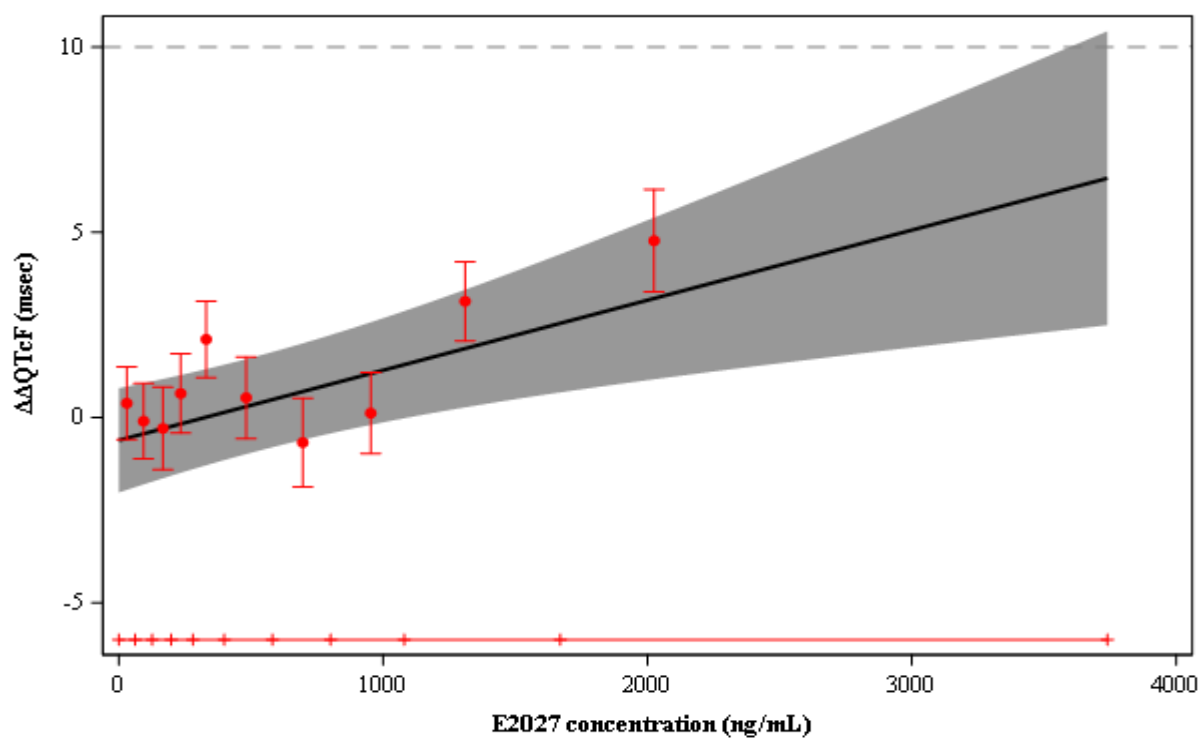
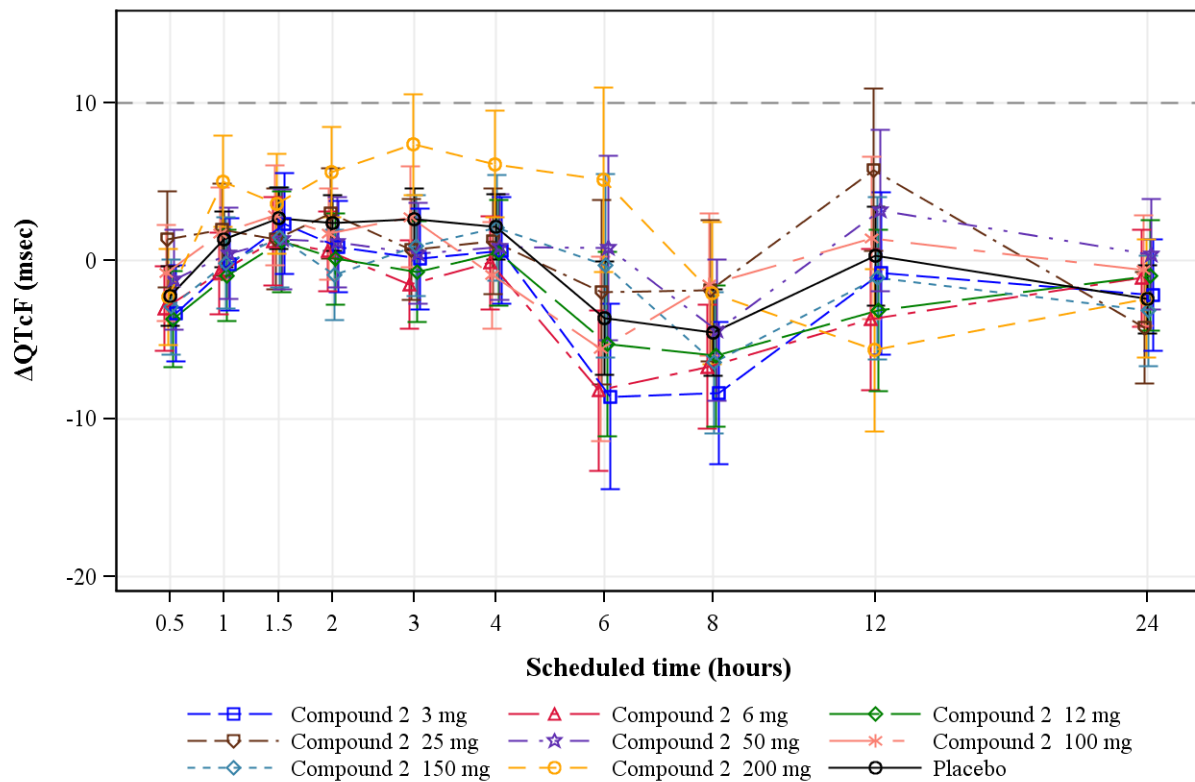


Figure 4

Panel A



Panel B

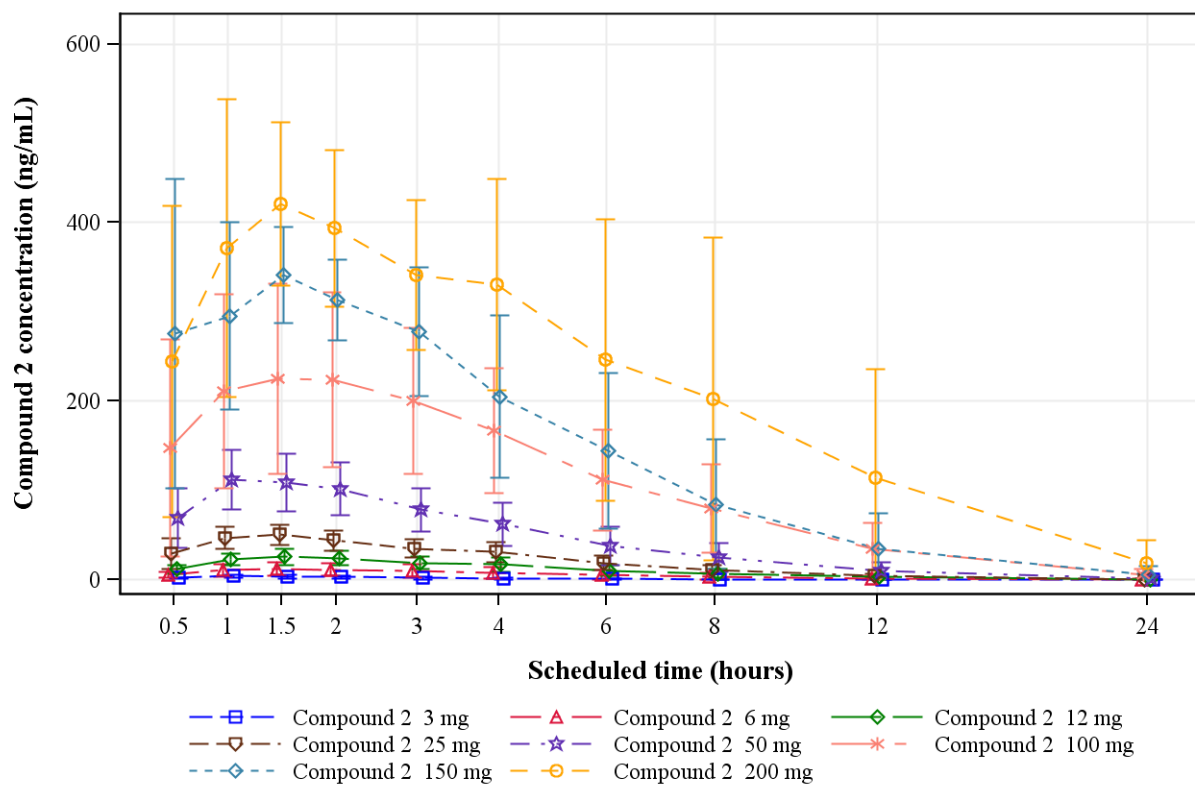
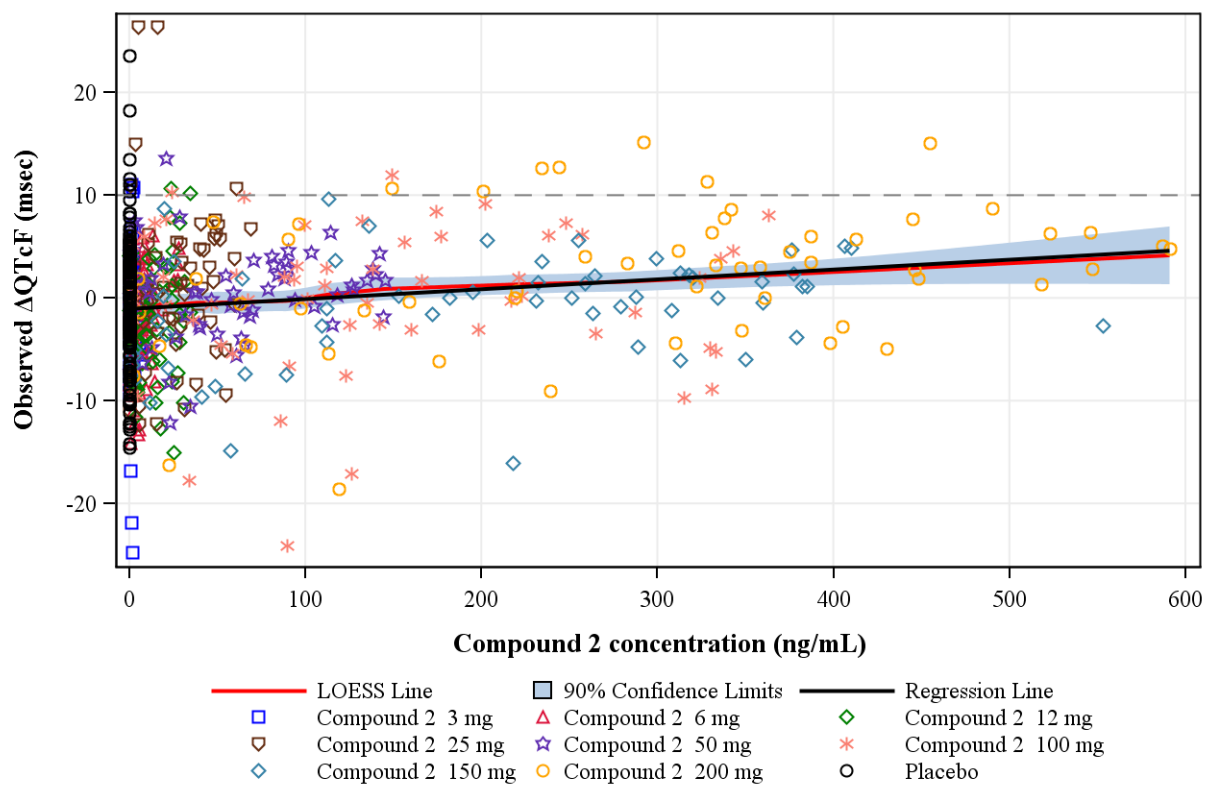


Figure 5

Panel A



Panel B

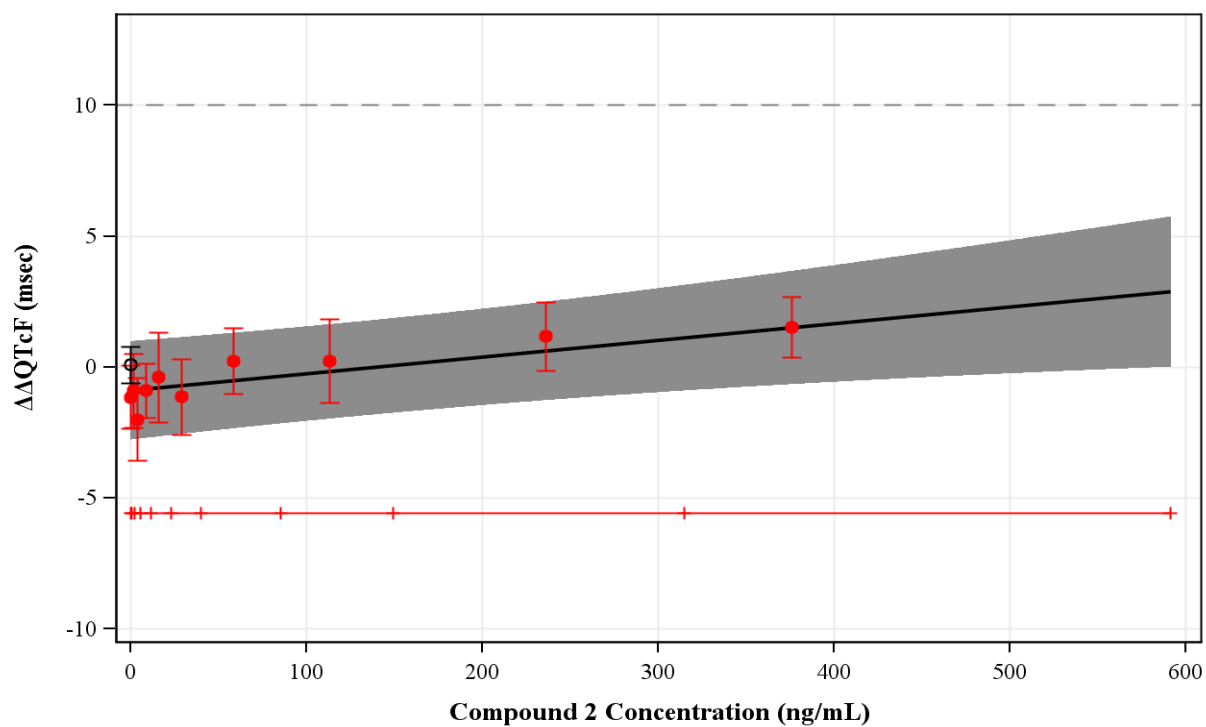
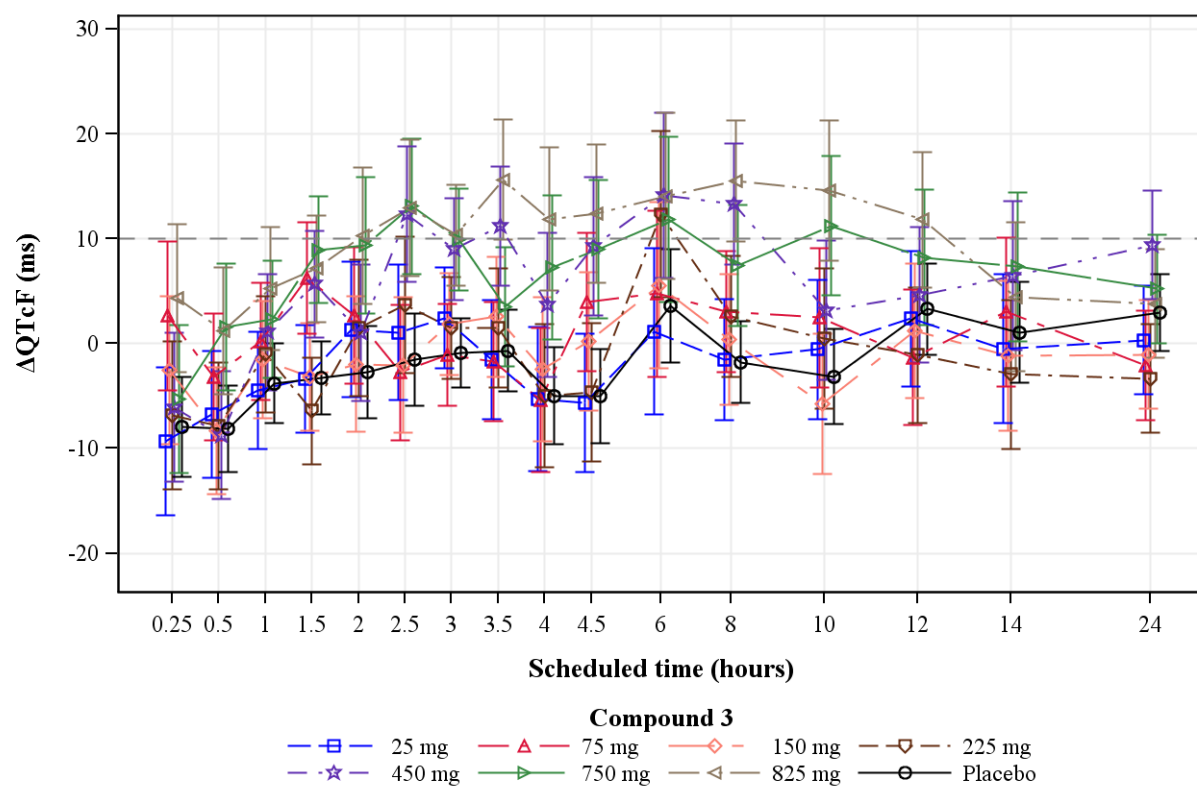
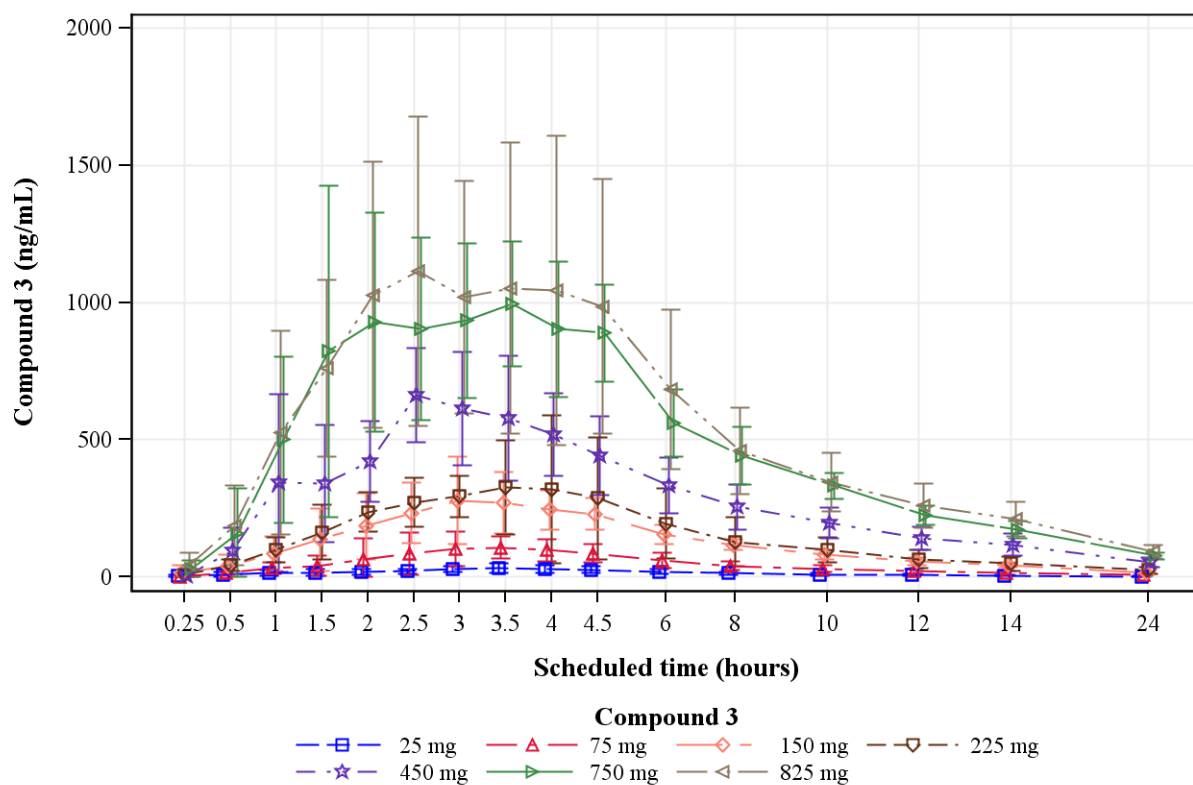


Figure 6
Panel A



Panel B



Panel C

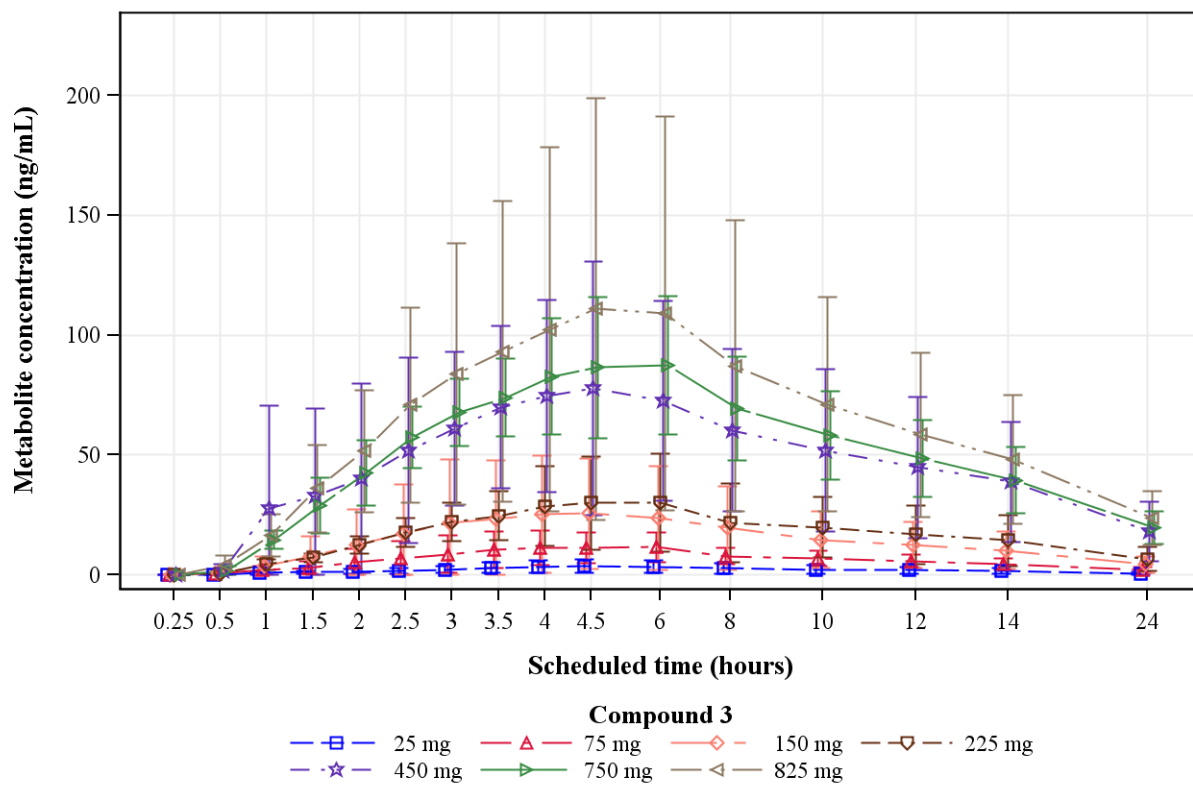
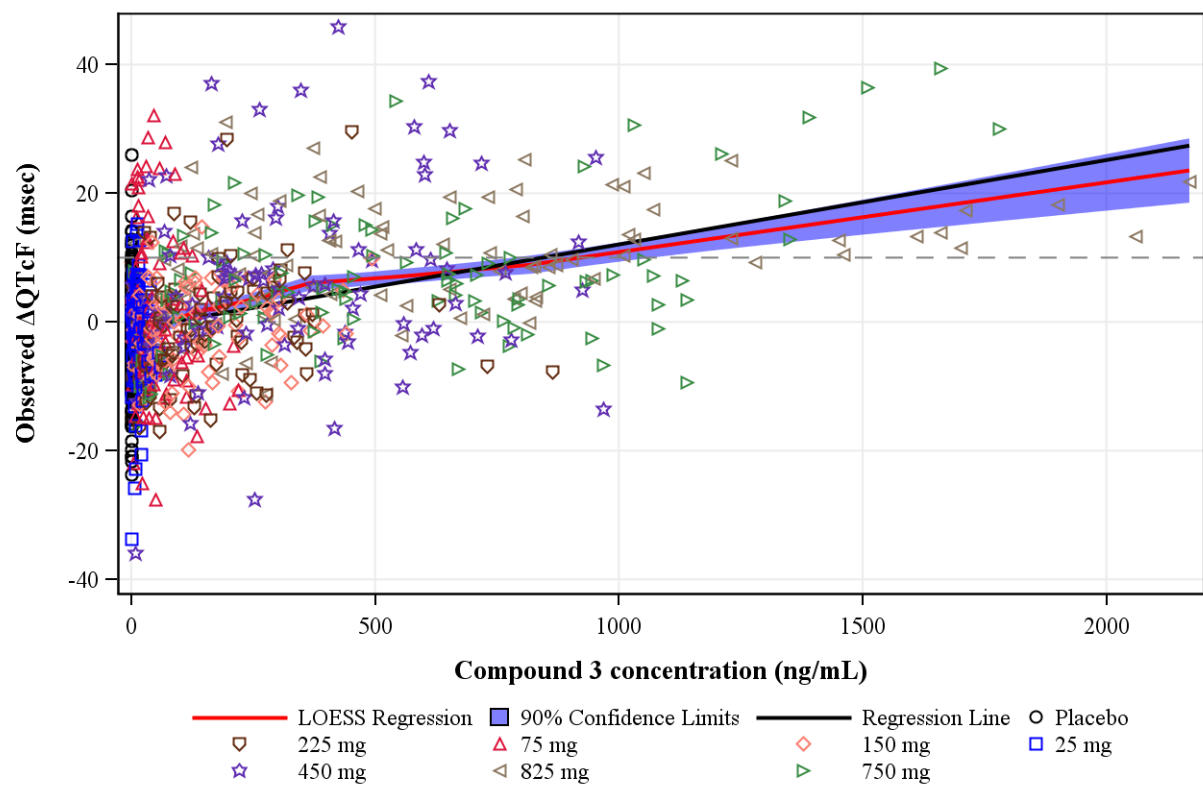
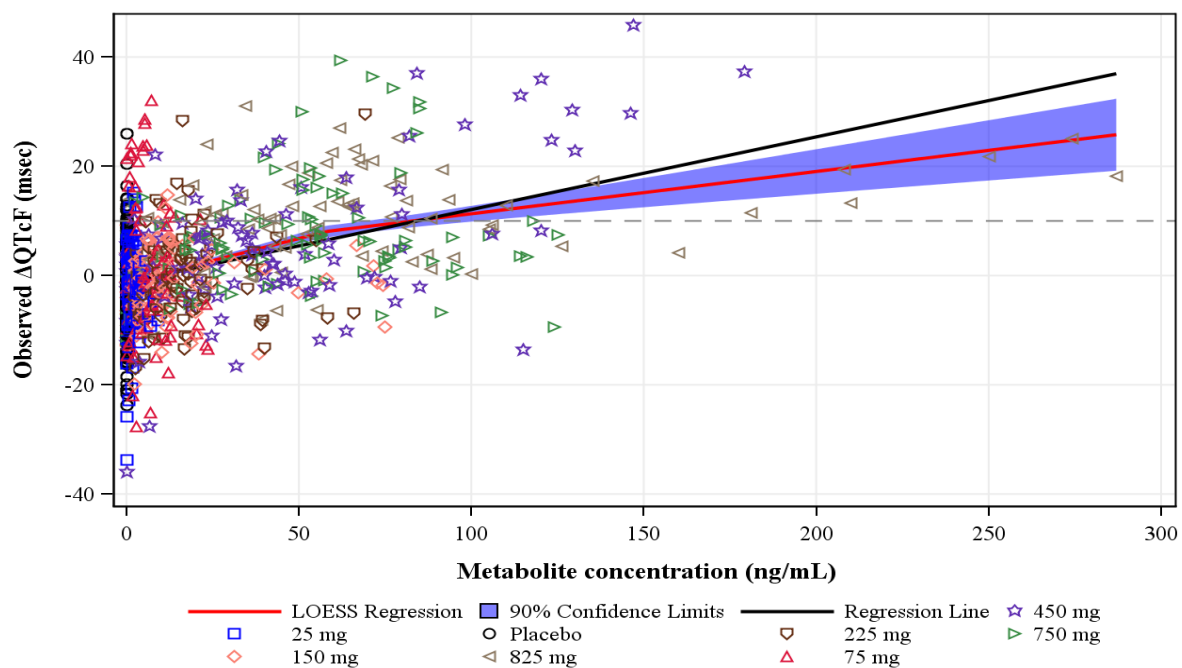


Figure 7

Panel A



Panel B



Panel C

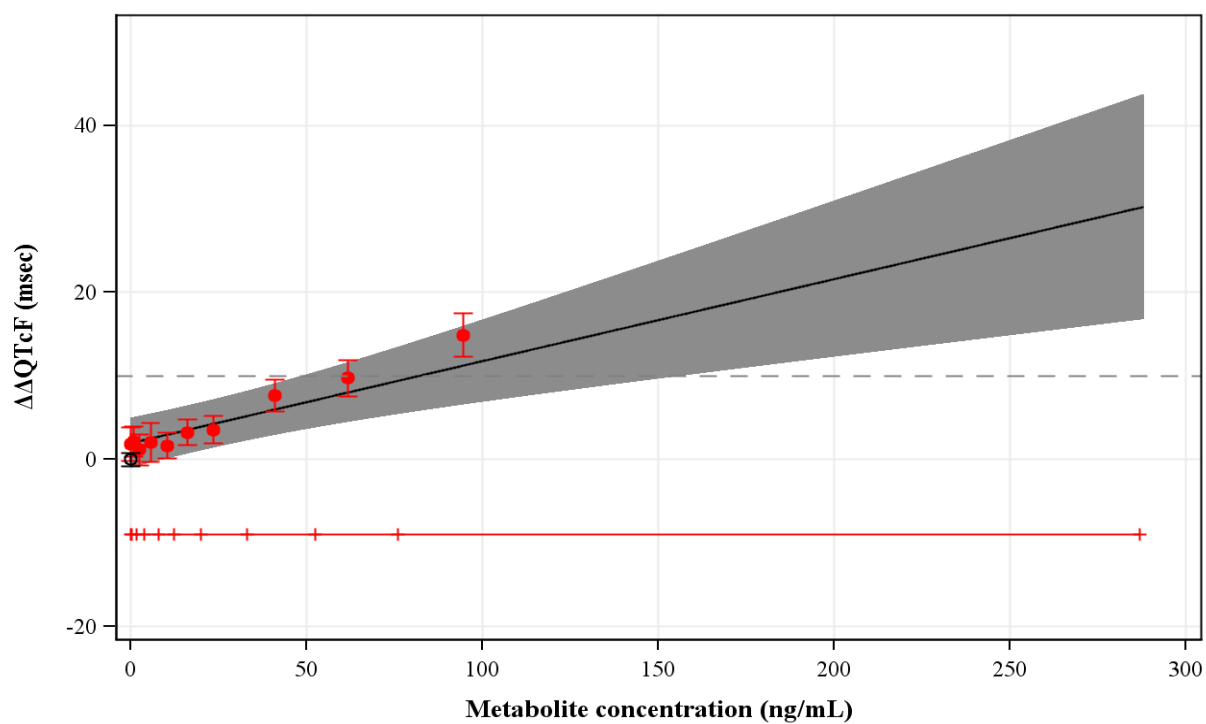
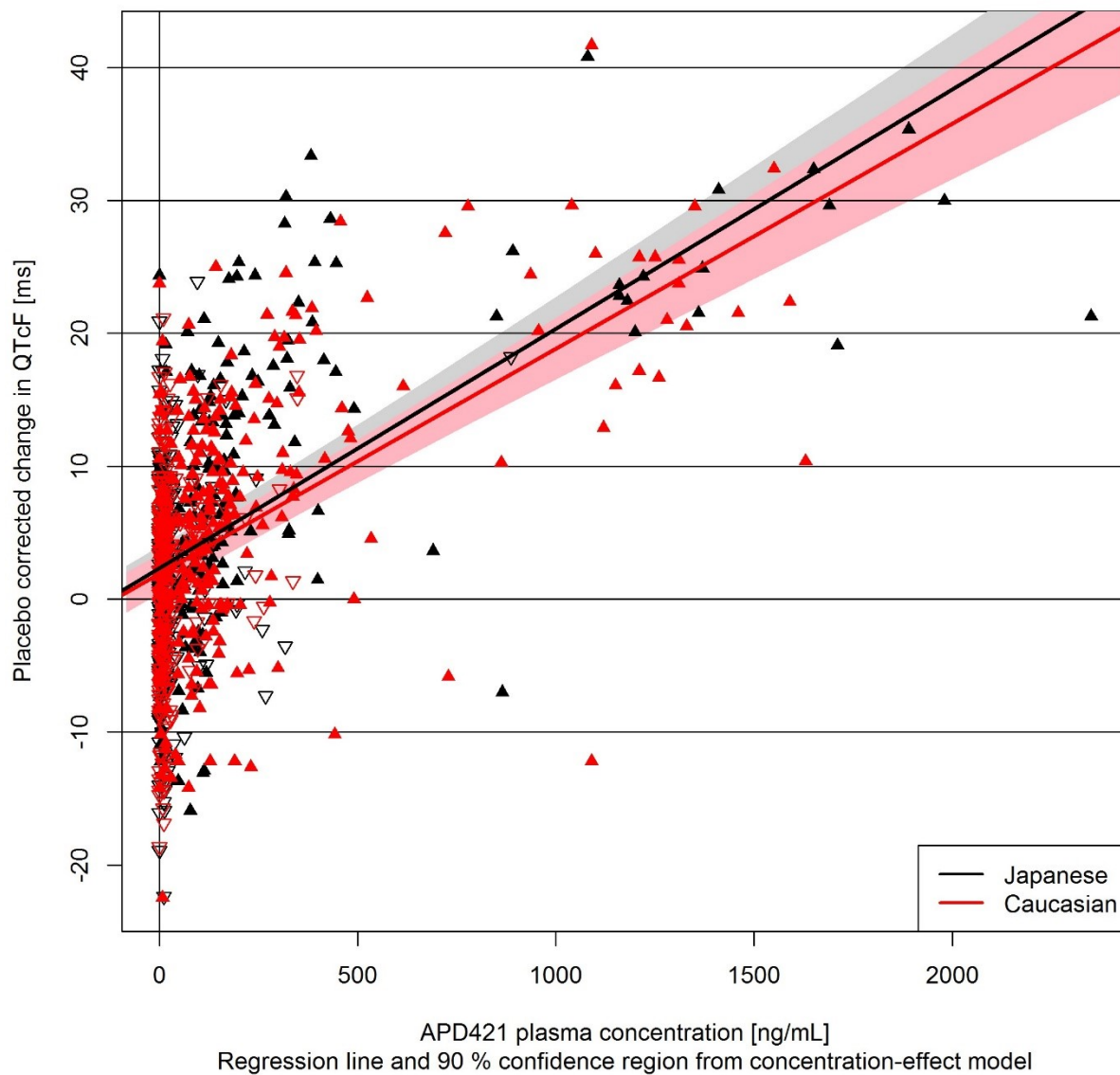


Figure 8
Panel A



Panel B

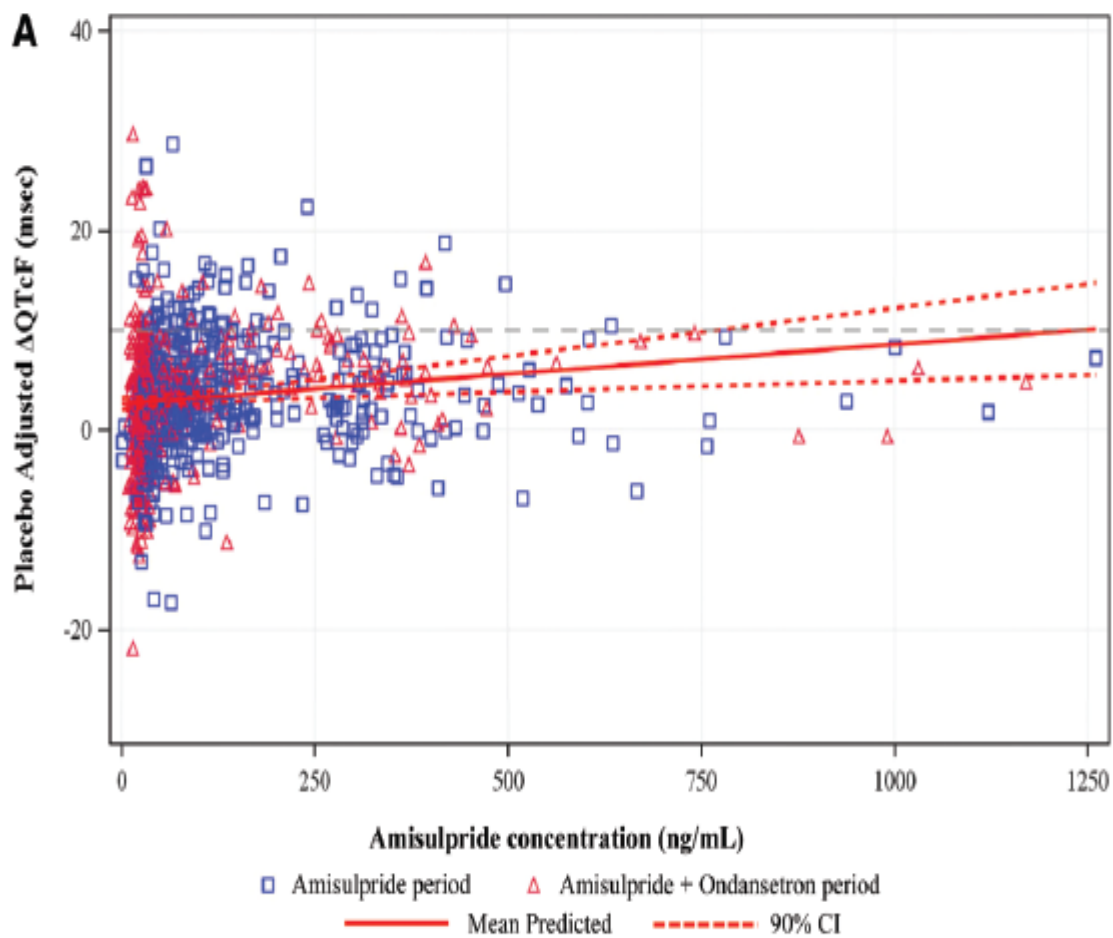
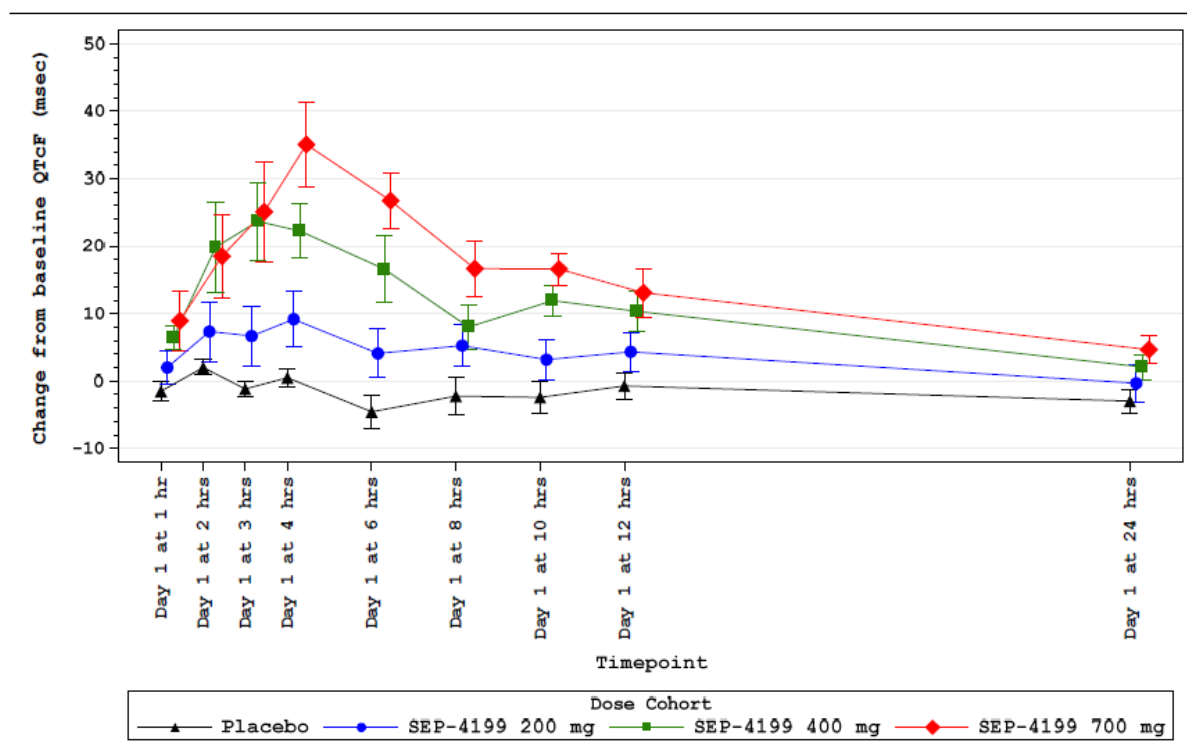


Figure 9
Panel A

Panel B

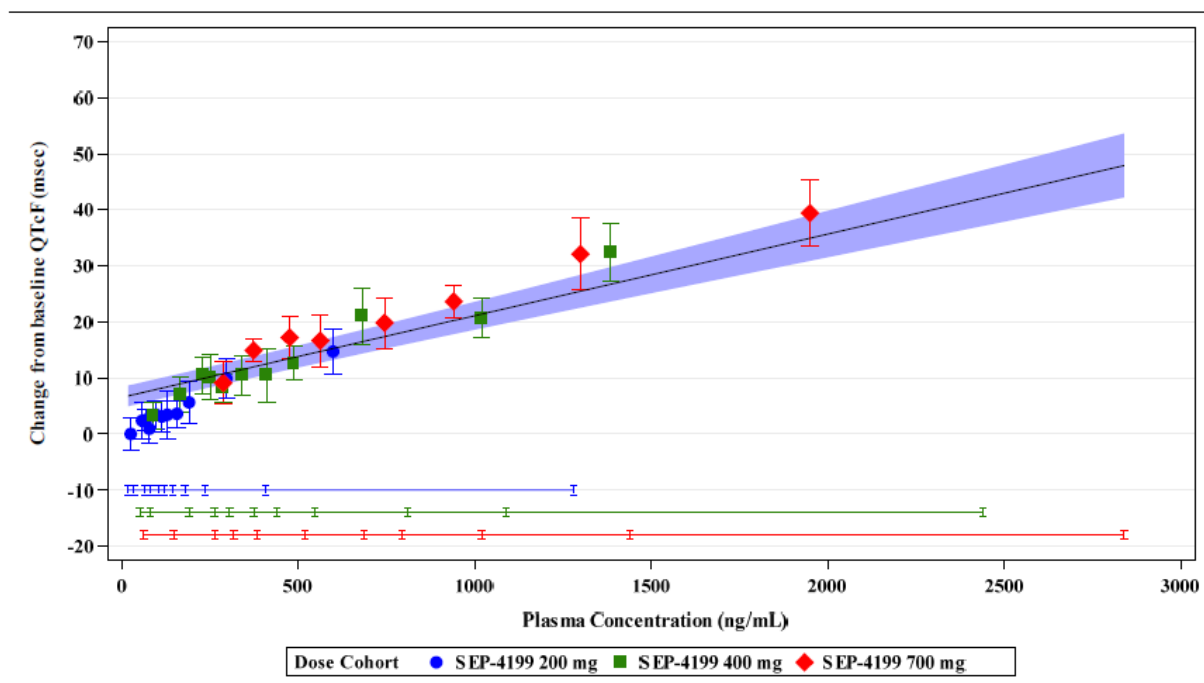
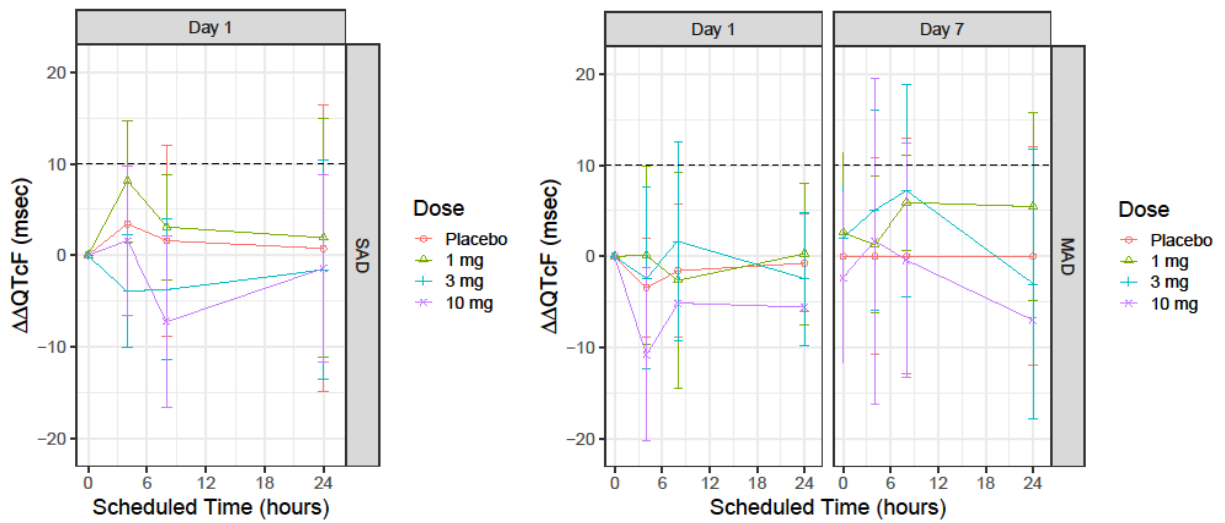
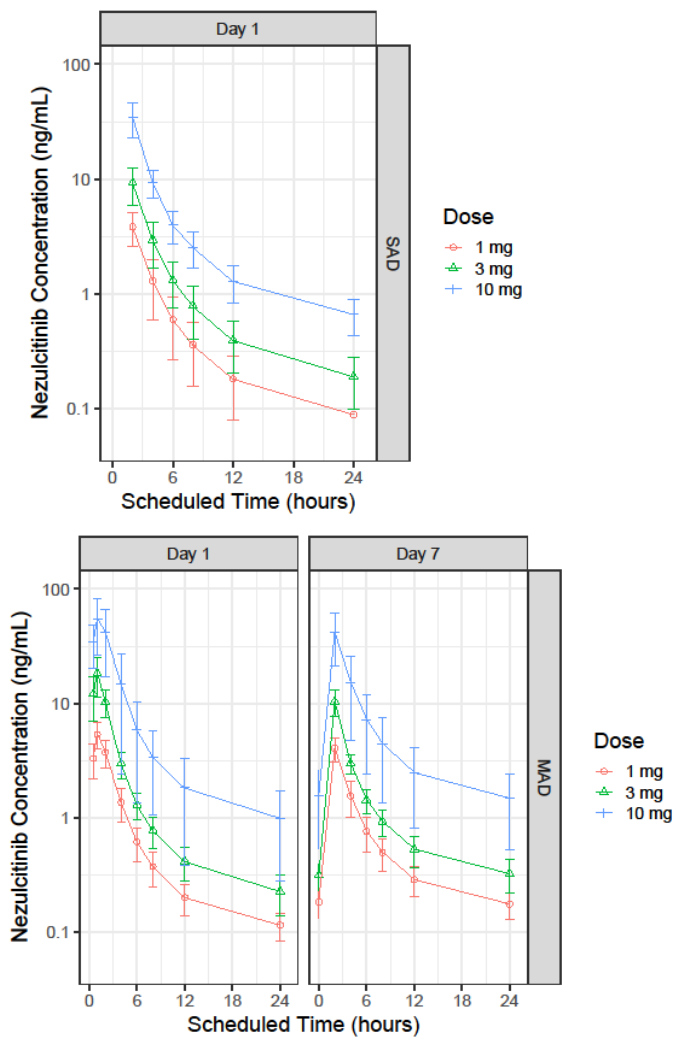


Figure 10

Panel A



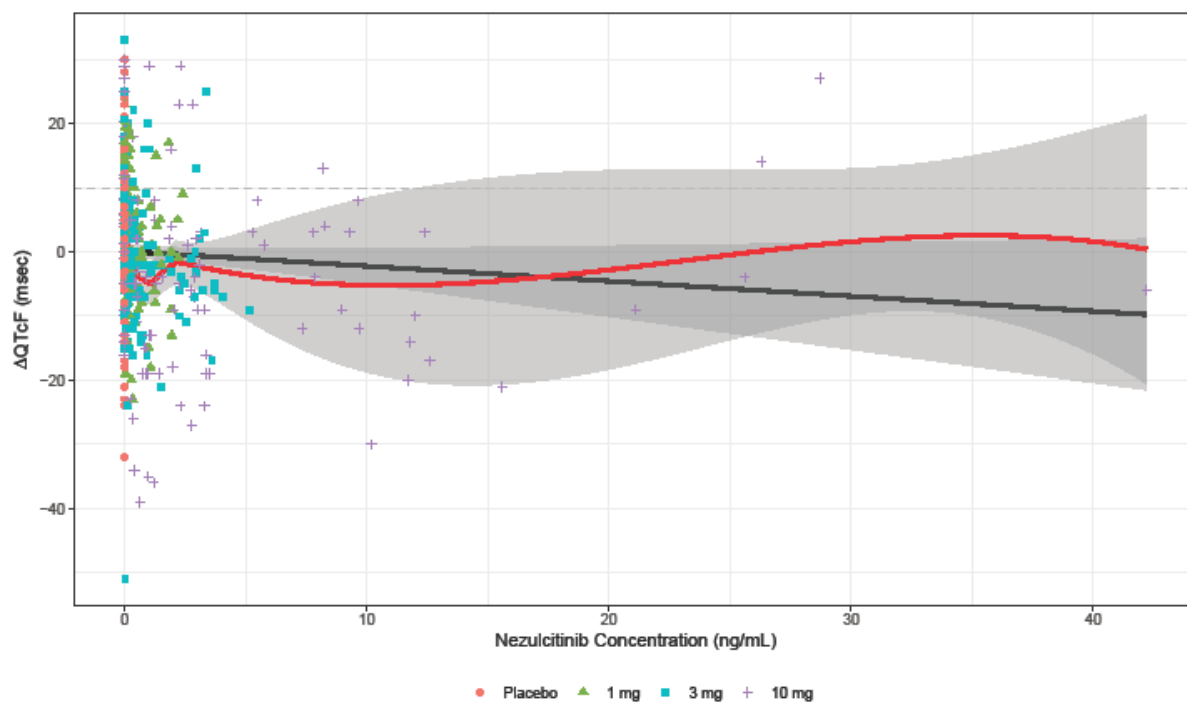
Panel B



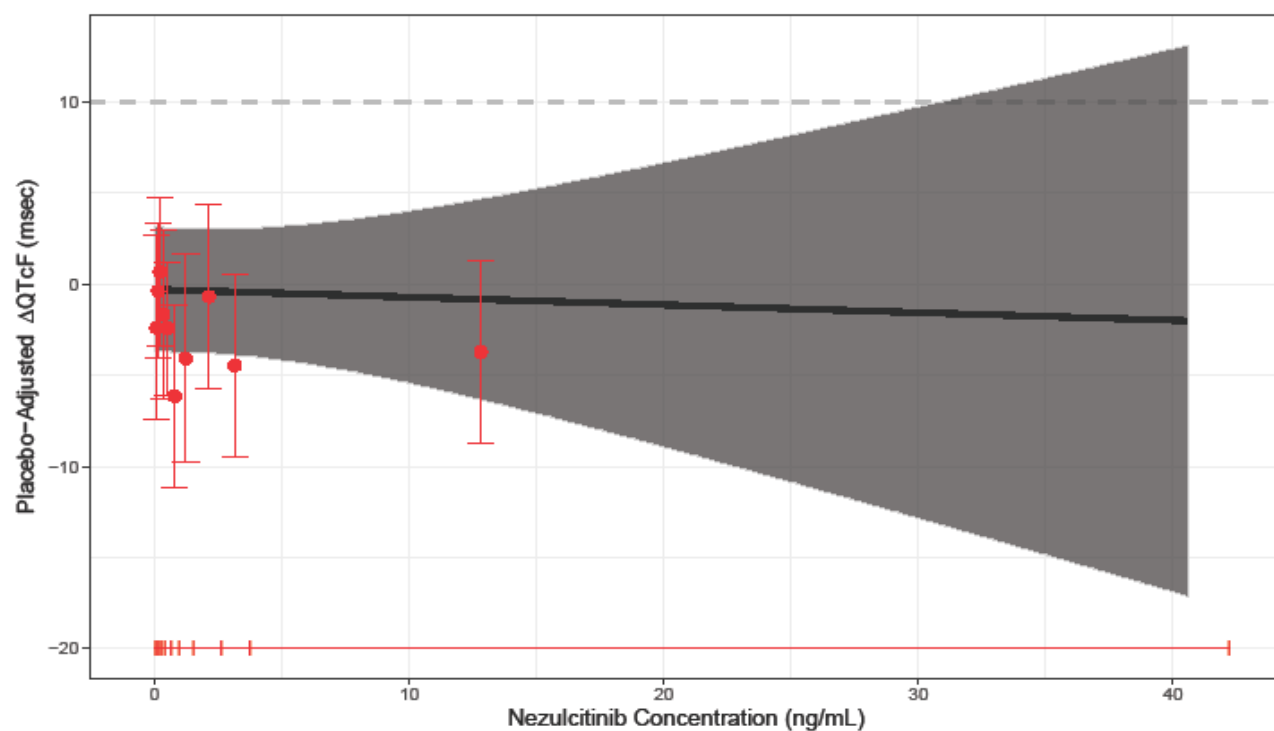
Accepted Article

Figure 11

Panel A



Panel B





About Clario

Clario generates the richest clinical evidence. Fusing our deep scientific expertise and global scale into the broadest endpoint technology platform, we empower our partners to transform lives.